Thermodynamic Balancing of the Humidification Dehumidification Desalination System by Mass Extraction and Injection

Citation: Narayan, G. Prakash, Karim M. Chehayeb, Ronan K. McGovern, Gregory P. Thiel, Syed M. Zubair, and John H. Lienhard V. "Thermodynamic Balancing of the Humidification Dehumidification Desalination System by Mass Extraction and Injection." International Journal of Heat and Mass Transfer 57, no. 2 (February 2013): 756–70.

As Published: http://dx.doi.org/10.1016/j.ijheatmasstransfer.2012.10.068

Publisher: Elsevier

Persistent URL: http://hdl.handle.net/1721.1/102568

Version: Author's final manuscript: final author's manuscript post peer review, without publisher's formatting or copy editing

Thermodynamic balancing of the humidification dehumidification desalination system by mass extraction and injection

G. Prakash Narayan[a,*], Karim M. Chehayeb[b,*], Ronan K. McGovern[a], Gregory P. Thiel[a], Syed M. Zubair[c], John H. Lienhard V[a,**]

[a] *Department of Mechanical Engineering, Massachusetts Institute of Technology, Cambridge, USA.*
[b] *Department of Mechanical Engineering, American University of Beirut, Beirut, Lebanon.*
[c] *Department of Mechanical Engineering, King Fahd University of Petroleum and Minerals, Dhahran, Saudi Arabia.*

Abstract

Humidification dehumidification (HDH) is a promising technology for small scale seawater desalination and has received widespread attention in recent years. The biggest roadblock to commercialization of this technology is its relatively high energy consumption. In this paper, we propose thermodynamic balancing of the humidifier or the dehumidifier through mass extraction and injection as a potential means of reducing the energy consumption of these systems. Balancing minimizes the entropy generation caused by imbalance in driving temperature and concentration differences. We outline a procedure to model the system, using on-design component variables, such that continuous or discrete extraction and/or injection of air from the humidifier to the dehumidifier or vice versa can be analyzed. We present an extraction profile (mass flow rate ratio versus non-dimensional position) in the dehumidifier and the humidifier for attaining close to complete thermodynamic reversibility in an HDH system with a 100% effective humidifier and dehumidifier. Further, we have examined in detail the effect of having finite-sized systems, of balancing the humidifier versus the dehumidifier, and that of the number of extractions.

Keywords: desalination, humidification, dehumidification, thermodynamic balancing, enthalpy pinch, remanent irreversiblity, entropy generation minimization, mass extraction, heat and mass exchangers

*Joint first authors
**Corresponding author
Email address: lienhard@mit.edu (John H. Lienhard V)

Nomenclature

Acronyms

GOR	Gained Output Ratio
HDH	Humidification Dehumidification
HE	Heat Exchanger
HME	Heat and Mass Exchanger
TTD	Terminal Temperature Difference

Symbols

c_p	specific heat capacity at constant pressure (J/kg·K)
$\dot{H}$	total enthalpy rate (W)
g	specific gibbs energy (J/kg)
h	specific enthalpy (J/kg)
h^*	specific enthalpy (J/kg dry air)
h_{fg}	specific enthalpy of vaporization (J/kg)
HCR	control volume based modified heat capacity rate ratio for HME devices (-)
m_r	water-to-air mass flow rate ratio (-)
$\dot{m}$	mass flow rate (kg/s)
N	number of extraction (-)
P	absolute pressure (Pa)
$\dot{Q}$	heat transfer rate (W)
RR	recovery ratio (%)
s	specific entropy (J/kg·K)
sal	feed water salinity (g/kg)
$\dot{S}_{gen}$	entropy generation rate (W/K)
T	temperature (°C)

Greek

Δ	difference or change
ε	energy based effectiveness (-)
Ψ	enthalpy pinch (kJ/kg dry air)
Ψ_{TD}	terminal enthalpy pinch (kJ/kg dry air)
η_{tvc}	reversible entrainment efficiency for a TVC(-)
η_e	isentropic efficiency for an expander (-)
ϕ	relative humidity (-)
ω	absolute humidity (kg water vapor per kg dry air)

Subscripts

a	humid air
c	cold stream
deh	dehumidifier
da	dry air
h	hot stream
hum	humidifier
HE	heat exchanger
in	entering
int	water-vapor interface
max	maximum
$local$	defined locally
out	leaving
pw	pure water
rev	reversible
w	seawater

Thermodynamic states

a	Seawater entering the dehumidifier
b	Preheated seawater leaving the dehumidifier
c	Seawater entering the humidifier from the brine heater
d	Brine reject leaving the humidifier
e	Moist air entering the dehumidifier
ex	Moist air state at which mass extraction and injection is carried out in single extraction cases
f	Relatively dry air entering the humidifier
g	Air at an arbitary intermediate location in the dehumidifier
i	Seawater at an arbitary intermediate location in the dehumidifier

1. Introduction

When finite time thermodynamics is used to optimize the energy efficiency of thermal systems, the optimal design is one which produces the minimum entropy within the constraints of the problem (such as fixed size or cost). In this study, we apply this well-established principle to the thermal design of combined heat and mass exchange devices (dehumidifiers, and humidifiers) for improving the energy efficiency of humidification dehumidification (HDH) desalination systems.

HDH is a distillation technology which operates using air as a carrier gas [1–3] to shuttle vapor and energy between the evaporation and condensation processes. The simplest version of this technology has a humidifier, a dehumidifier, and a heater to heat the seawater stream. Studies have been conducted on the effect of entropy generation on the thermal design of the HDH system [4, 5] and it has been found that reducing the total entropy generated (per unit amount of water distilled) improves the energy efficiency (measured in terms of the gained-output-ratio or GOR). It has also been reported that incorporating mass extractions and injections to vary the water-to-air mass flow rate ratio in the combined heat and mass transfer devices (like the humidifier and the dehumidifier) can potentially help in reducing entropy production in those devices [6]. In the present study, we report a comprehensive thermodynamic analysis to understand how to design for the aforementioned mass extractions and injections in the HDH system. This design (discussed in the succeeding sections) draws upon the fundamental observation that there is a single value of water-to-air mass flow rate ratio (for any given boundary conditions and component effectivenesses) at which the system performs optimally [3].

A schematic diagram of an embodiment of the HDH system with mass extractions and injections is shown in Fig. 1. The system shown here is a water-heated, closed-air, open-water system with three air extractions from the humidifier into the dehumidifier. States a to d are used to represent various states of the seawater stream and states e and f represent that of moist air before and after dehumidification. There are several other embodiments of the

system possible based on the various classifications of HDH listed by Narayan et al. [1].

[Figure 1 about here.]

1.1. Literature review

Even though there has been no clear conceptual understanding of how the thermal design of HDH systems with mass extraction/injection should be carried out, a small number of studies in literature discuss limited performance characteristics of these systems. Müller-Holst pioneered the thermal balancing of HDH systems by proposing to balance the stream-to-stream temperature difference in the HME devices by 'continuous' variation of the water-to-air mass flow rate ratio [7, 8]. The moist air in the proposed system was circulated using natural convection and the mass flow rate of this stream was varied by strategically placed extraction and injection ports in the humidifier and the dehumidifiers respectively. An optimized thermal energy consumption of 120 kWh/m^3 ($\approx$ 450 kJ/kg) was reported for this system.

Zamen et al. [9] reported a novel 'multi-stage process' which was designed for varying the water-to-air mass flow rate ratio. This was achieved by having multiple stages of humidification and dehumidification in series with separate air flow for each stage and a common brine flow. A similar design was also reported by Schlickum [10] & Hou [11]. Zamen et al. [9] used a temperature pinch (defined as the minimum stream-to-stream temperature difference in the HME device) between the water and the air streams to define the performance of the system. For a four stage system with component pinch of 4°C, at a feed water temperature of 20°C and a top brine temperature of 70°C, Zamen et al. reported an energy consumption of slightly less than 800 kJ/kg.

Brendel [12, 13] invented a novel forced convection driven HDH system in which water was extracted from several locations in between the humidifier and sent to corresponding locations in the dehumidifier. This was done such that the temperature profiles were balanced (as was the case with Zamen et al. [9]). In a recent publication, Thiel and Lienhard [14] have shown

that in order to attain the thermodynamic optimum in HME devices we have to consider both temperature, and concentration profiles and that the optimum lies closer to a balanced humidity profile than a balanced temperature profile. This finding is discussed further in Sec. 2.

Younis et al. [15] studied air extraction and injection in forced convection driven HDH systems. They found that having two extractions of air from the humidifier to the dehumidifier decreased the energy consumption of the system to 800 kJ/kg. Like in several other publications [7, 9, 12, 16], they used enthalpy-temperature diagrams to demonstrate the effect of extraction on HDH system design. McGovern et al. [16] pinoored the use of the graphical technique and highlighted the important approximations that need to be made to use it for HDH system design.

Bourouni [2] in a review of the HDH technology reported that a few other authors [17] studied air extractions in HDH systems and reported performance enhancements as a result of such a design. However, these studies are dated and no longer available in open literature.

1.2. Goals of the current study

Despite all of the aforementioned publications on the subject, several questions remain unanswered. We address them in a comprehensive manner in the current publication. These include: (1) evaluating the upper limit on performance of a HDH system with mass extractions and injections; (2) developing design algorithms to completely balance HME devices and HDH systems; (3) understanding the effect of balancing the humidifier as opposed to balancing the dehumidifier on the performance of the HDH system; and (4) examining the effect of number of extractions on the HDH system.

2. Thermal balancing in combined heat and mass transfer devices

A major portion of the entropy produced in the HDH system is due to the heat and mass transfer mechanisms occuring in the humidifier and the dehumidifier. Mistry et al. [4] demonstrated that at an optimal water-to-air mass flow rate ratio, 70% or more of all the

entropy produced in the water-heated HDH system was produced in the humidifier and the dehumidifier. In order to reduce the entropy production of the system we have to address the entropy produced in the humidifier and dehumidifier. In this section, we revisit the algorithm (previously developed [6]) for control volume balancing of HME devices and extend it to continuous and discrete balancing of these devices using mass extractions and injections. We also propose an appropriate alternative to the 'component effectiveness' [18–20] and the 'temperature pinch' [9, 11, 16] techniques of modeling HME devices.

2.1. 'Control volume' balancing

To understand thermodynamic balancing in HME devices let us consider the simpler case of a heat exchanger first. In the limit of infinite heat transfer area, the entropy generation rate in this device will be entirely due to what is known as thermal imbalance or remanent irreversibility. This is associated with conditions at which the heat capacity rate of the streams exchanging heat are not equal [21]. In other words, a heat exchanger (with constant heat heat capacity for the fluid streams) is said to be thermally 'balanced' (with zero remanent irreversibility) at a heat capacity rate ratio of one. This concept of thermodynamic balancing, very well known for heat exchangers, was recently extended to HME devices [6].

In order to define a thermally 'balanced' state in HME devices, a modified heat capacity rate ratio for combined heat and mass exchange was defined by analogy to heat exchangers as the ratio of the maximum change in total enthalpy rate of the cold stream to that of the hot stream. The maximum changes are defined by defining the ideal states that either stream can reach at the outlet of the device. For example, the ideal state that a cold stream can reach at the outlet will be at the inlet temperature of the hot stream and that a hot stream can reach at the outlet will be at the inlet temperature of the cold stream. The physics behind this definition is explained in a previous publication [6].

$$\mathrm{HCR} = \left(\frac{\Delta \dot{H}_{\mathrm{max},c}}{\Delta \dot{H}_{\mathrm{max},h}} \right) \tag{1}$$

It was shown previously that at fixed inlet conditions and effectiveness, the entropy generation of a combined heat and mass exchange device is minimized when the modified heat capacity rate ratio (HCR) is equal to unity [6]. Further, a recent study [14] has shown that for a fixed heat transfer rate, condensation rate, and HME size, the entropy generation in a dehumidifier approaches a minimum when HCR approaches unity. Thus, we could say that HCR being unity defines the balanced state for HME devices irrespective of whether it is a fixed effectiveness or a fixed hardware condition. However, this is a 'control volume' balanced state wherein the design does not include mass extractions and injections. We will now try to extend the control volume concept to that of complete thermodynamic balancing in HME devices by variation of water-to-air mass flow rate ratio along the process path.

2.2. Enthalpy pinch: novel parameter to define performance of HME device

To clearly visualize the simultaneous heat and mass transfer process, we consider the example of a dehumidifier and plot a temperature versus enthalpy diagram (Fig. 2). In section 4 of a recent publication [16], we explained in detail the various approximations involved in such graphical representations. The approximations involved in Fig. 2 are also summarized in appendix A of the present paper.

[Figure 2 about here.]

In Fig. 2, e to f represents the process path for dehumidification of the moist air and a to b represents the process path for energy capture by the seawater stream. f′ and b′ represent the hypothetical ideal states the moist air and water stream would have, respectively, reached if the dehumidifier had been of infinite size. Hence, $h^*|_f - h^*|_{f'}$ (represented as Ψ_h) and $h^*|_{b'} - h^*|_b$ (represented as Ψ_c) is the loss in enthalpy rates (per unit amount of dry air circulated in the system) because of having a "finite-sized" HME device. This is the loss that we cannot reduce by thermal balancing of the device at a control volume balanced condition (without increasing the area associated with the heat and mass transfer in the device). For a given device, this is the loss that represents the energy effectiveness of the device (ε) and

is directly related to conventional definition of an exchanger effectiveness definition. This definition of effectiveness [18, 22] for a heat and mass exchanger is given as:

$$\varepsilon = \frac{\Delta \dot{H}}{\Delta \dot{H}_{\max}} \tag{2}$$

The maximum change in total enthalpy rate is the minimum of that for the cold and the hot stream.

$$\Delta \dot{H}_{\max} = \min(\Delta \dot{H}_{\max,c}, \Delta \dot{H}_{\max,h}) \tag{3}$$

McGovern et al. [16] proposed that it is advantageous to normalize enthapy rates by the amount of dry air flowing through the system for easy representation of the thermodynamic processes in enthalpy versus temperature diagrams. We use this concept throughout this publication and derive the following equation from Eq. (2) by dividing the numerator and the denominator by the mass flow rate of dry air ($\dot{m}_{da}$).

$$\varepsilon = \frac{\Delta h^*}{\Delta h^*_{\max}} \tag{4}$$

$$= \frac{\Delta h^*}{\Delta h^* + \Psi_{TD}} \tag{5}$$

Ψ_{TD} is the loss in enthalpy rates at terminal locations because of having a "finite-sized" HME device and is defined as follows:

$$\Psi_{TD} = \min\left(\frac{\Delta \dot{H}_{\max,c}}{\dot{m}_{da}} - \Delta h^*, \frac{\Delta \dot{H}_{\max,h}}{\dot{m}_{da}} - \Delta h^*\right) \tag{6}$$

$$= \min(\Psi_c, \Psi_h) \tag{7}$$

In the case of a heat exchanger, Ψ_{TD} will be analogous to the minimum terminal stream-to-stream temperature difference (TTD). However, TTD is seldom used to define performance of a heat exchanger in thermodynamic analyses; the temperature pinch is the commonly used parameter. The difference is that pinch is the minimum stream-to-stream temperature

difference at any point in the heat exchanger and not just at the terminal locations. Like temperature pinch, Ψ can be defined as the minimum loss in enthalpy rate due to a finite device size at any point in the exchanger and not just at the terminal locations. This is accomplished, as shown in Fig. 3, by considering infinitely small control volumes represented by just two states (g for air and i for water). We can define the ideal states for each of these real states as g′ and i′. The local Ψ at this location can be defined as the minimum of $h|_{i'} - h|_i$ (represented as Ψ_2) and $h|_g - h|_{g'}$ (represented as Ψ_1). Thus, the general definition of Ψ will be as follows:

$$\Psi = \min_{local}(\Delta h^*_{\max} - \Delta h^*) \tag{8}$$

Hence, based on the arguments presented in this section, we can say that Ψ for an HME device is analogous to temperature pinch for an HE, and it can be called the 'enthalpy pinch'. We recommend that, because of the presence of the concentration difference as the driving force for mass transfer in HME devices, a temperature pinch or a terminal temperature difference should not be used when defining the performance of the device.

[Figure 3 about here.]

The energy effectiveness is another commonly used performance metric for HEs [22] and HMEs [18]. But, this is a control volume parameter and accounts for only terminal differences. In order to design for balancing, we need to consider local differences. Consider the temperature profile of a humidification process as shown in Fig. 4: the 'pinch' point does not occur at the terminal locations but rather at an intermediate point. This behaviour is not captured if we define the performance of the device by an energy effectiveness. In the extreme case, as demonstrated by Miller [5], high values of effectiveness for the humidifier could lead to an internal temperature and concentration cross. Ψ does not have this problem since it is a local parameter and is, hence, used to define the performance of HME devices (humidifiers and dehumidifiers) in this publication.

[Figure 4 about here.]

2.3. Mass extractions and/or injections based balancing

As described in Sec. 2.1, a value of unity for the modified heat capacity rate ratio defines a thermally balanced state for a control volume without extractions. For such a case HCR is not equal to unity at all locations in the device. With mass extractions we can vary the slope of the water line such that HCR is one throughout the device. This is the operating condition at which the HME device is completely balanced. We rewrite the expression for HCR in terms of Ψ_c and Ψ_h to understand this concept.

$$\text{HCR} = \frac{\Delta \dot{H}_{\max,c}}{\Delta \dot{H}_{\max,h}} \tag{9}$$

$$= \frac{\Delta h^* + \Psi_c}{\Delta h^* + \Psi_h} \tag{10}$$

$$\text{when HCR=1 for the CV,} \quad \Psi_{TD,c} = \Psi_{TD,h} \tag{11}$$

$$\text{when HCR=1 at all locations,} \quad \Psi = \text{constant} \tag{12}$$

To vary the water-to-air mass flow rate ratio such that HCR=1 at every location in the device (or conversely $\Psi =$ constant at every point) we need extractions or injections at every point (the number of extractions of injections approach infinity). We call this "continuous thermodynamic balancing". Even though this has theoretical significance in understanding systems with mass extraction and injection, in practice it will be difficult to achieve. Hence, we also evaluate balancing an HME device with a finite number of extractions. (In the cases reported in this paper, we investigate a single extraction.)

As can be understood by looking at Figs. 2 and 3, in a 'control volume' balanced dehumidifier without extractions, the local Ψ is minimum at the two terminal locations (also see Eq. 11), and at all intermediate points it is higher. This results from the nature of the temperature-enthalpy diagram as discussed in more detail in Sec. 3. The local variation of

Ψ in the control volume balanced case is illustrated in Fig. 5[1]. As may be observed from the figure, a single extraction brings Ψ to a minimum value at one intermediate location (or conversely brings HCR = 1 at that location and the two terminal ones). In the case of the number of extractions approaching infinity, local value of Ψ can be minimum and constant throughout the length of the device (Eq. 12). The direction of extraction of air is to the dehumidifier. Since, we need to vary the water-to-air mass rate ratio to balance the device (and not individual mass flow rates) we can equivalently extract water from the (counterflow) dehumidifier.

[Figure 5 about here.]

Figure 6 illustrates the effect of continuous and single extraction on the total irreversiblity in the dehumidifier. The entropy produced per unit amount of water condensed is reduced to a quarter with continuous extraction and to $3/5^{\text{th}}$ with a single extraction. This is representative of an optimal case. Such a large reduction demonstrates the importance of thermodynamic balancing for heat and mass exchangers.

[Figure 6 about here.]

2.4. Functional form for continuous thermodynamic balancing

Considering Eq. 12, we can write down the closed form expressions [Eqs. (13–18)] for the temperature and humidity ratio profiles for the fluid streams in a completely balanced dehumidifier and humidifier. If the process path for air (represented in an enthalpy-temperature diagram) follows a function ξ (Eq. 13) then the mass flow rate ratio is varied in the dehumidifier such that the seawater process path is the same function of enthalpy, but shifted by Ψ (Eq. 15). A similar shift in the enthalpy is also followed in the humidity profile (Eqns. 14 & 16).

[1]For the x-axis in Fig. 5, the specific enthapy per kg of dry air (used to describe the control volume location in Figs.(2-3)) is normalised by the total heat duty (Δh^*). This convention is used in the rest of the publication.

$$T_a = \xi(h^*) \tag{13}$$

$$\omega = \eta(h^*) \tag{14}$$

$$T_w = \xi(h^* - \Psi) \tag{15}$$

$$\omega_{int} = \eta(h^* - \Psi) \tag{16}$$

[Figure 7 about here.]

An example of a temperature and humidity profile in a dehumidifier with continuous extraction is illustrated in Fig. 7. It can be seen from Fig. 7 that a dehumidifier with continuous mass extractions (such that HCR = 1 throughout the device) has a profile close to a constant driving humidity difference[2] rather than a constant temperature difference. This is a very significant conclusion and is further corroborated by results obtained from a transport process analysis by Thiel & Lienhard [14]. It also leads us to conclude that balancing for temperature differences alone (as carried out by all previous studies reviewed in Sec. 1.1) will not lead to a thermodynamic optimum.

For a completely balanced humidification device, the concept is similar. For a moist air line represented by Eq. 13 & 14, the humidifier water lines will be given by:

$$T_w = \xi(h^* + \Psi) \tag{17}$$

$$\omega_{int} = \eta(h^* + \Psi) \tag{18}$$

The complete extraction profiles can be obtained by only varying the water-to-air mass flow rate ratio. This can be done by continuous extraction or injection of either the air or the water (or both) from or into the HME device.

[2]Driving humidity difference is calculated as the difference in the local humidity ratio of the bulk air stream (avluate at a bulk temperature) and the humidity ratio of the interface (evaluated as saturated at the interface temperature).

3. Modeling of HDH systems

In the current section, we use the concepts of thermodynamic balancing developed for HME devices and apply them to the HDH system design. An embodiment of the system under study is illustrated in Fig. 1.

3.1. System without extractions

A temperature-enthalpy diagram for the HDH system without extractions (illustrated earlier in Fig. 1) is shown in Fig. 8. The process line for the air is represented by the saturation line 'ef' in the humidifier and the dehumidifier. The uncertainity in the calculated performance of the HDH system as a result of the approximation that air is saturated all along its process path is small and is discussed in detail in Sec. 4.3. The seawater process line is represented by 'ab' in the humidifier, by 'bc' in the heater and by 'cd' in the dehumidifier.

A detailed algorithm to design this system using the top brine temperature, the feed water temperature and the component enthalpy pinches as input variables is elucidated in Fig. 17 of Appendix B. The design of the HDH system using temperature-enthalpy diagrams was also previously discussed by other researchers [7, 9, 12, 16]. A temperature pinch was used in that study instead of an enthalpy pinch used in the current publication. As illustrated in Fig. 17, the solution is iterative and the thermophysical properties are evaluated as described in Sec. 3.4.

[Figure 8 about here.]

Other than the energy and mass conservation equations described in previous publications [3, 18], the understanding that the slope of the water line in the temperature versus enthalpy diagram can be used to evaluate the mass flow rate ratio at any given point in the HME devices is important to the analysis:

$$slope = \frac{dT_w}{dh^*} = \frac{1}{m_r c_{p,w}} \tag{19}$$

Further, the entropy of the varies states evaluated using the temperature-enthalpy diagram may be used to evaluate the mass flow rate in the humidification and the dehumidification devices.

3.2. System with infinite extractions and injections

Equations (13-18) are fundamental to designing systems with infinite extraction such that the remanent irreversibility in one of the humidifier or the dehumidifier is zero. Fig. 9 illustrates the application of the aforementioned equations in system design via temperature versus location diagrams. From a pinch point perspective, the temperature pinch in the humidifier and the dehumidifier are at different terminal ends in the 'dehumidifier balanced' and 'humidifier balanced cases'. The enthalpy pinch, however, is minimum and constant at all points in the dehumidifier and humidifier in the two respective cases.

[Figure 9 about here.]

The detailed procedure to model the system with infinite extractions illustrated in Fig. 18 of Appendix B. In developing this procedure we have put in a place a constraint that the state (temperature and humidity) of the injected stream is the same as the stream it is injected into. This is done to avoid generating entropy because of mixing of streams at dissimilar states. Further, it is important to note that air in the dehumidifier has the same inlet and outlet temperature and humidity unlike water which has a different streamwise temperature in the humidifier and the dehumidifier (because of presence of the heater). Thus for the HDH system under study in this publication, it is not possible to perform water extractions and injections without either generating entropy due to mixing or without limiting the number of extractions. Hence, air extraction is studied in this publication.

3.3. System with a single extraction and injection

It is, perhaps, more practical to apply a finite number of extractions and injections in the HDH system. Hence, we study the effect of a single extraction in this publication along

with that of infinite extractions. Fig. 10 illustrates a temperature profile of a system with a single extraction and injection. In the illustrated case, the air was extracted from the humidifier at the state 'ex' and injected in a corresponding location in the dehumidifier with the same state 'ex' to avoid generating entropy during the process of injection. This criteria for extraction is applied for all the cases reported in this paper since it helps us study the effect of thermodynamic balancing, independently, by separating out the effects of a temperature and/or a concentration mismatch between the injected stream and the fluid stream passing through the HME device (which when present can make it hard to quantify the reduction in entropy generated due to balancing alone).

[Figure 10 about here.]

The detailed procedure to model the system with a single air extraction and injection is illustrated in Fig. 19 of Appendix B.

3.4. Property packages

- The thermophysical properties of seawater were evaluated using the correlations presentated by Sharqawy et al. [23].
- Thermophysical properties of pure water are evaluated using the IAPWS (International Association for Properties of Water and Steam) 1995 Formulation [24].
- Moist air properties are evaluated assuming an ideal mixture of air and steam using the formulations presented by Hyland and Wexler [25].
- Moist air properties thus calculated are in close agreement with the data presented in ASHRAE Fundamentals [26] and pure water properties are equivalent to those found in NIST's property package, REFPROP [27].

4. Results and discussion

In this section, we investigate the effect thermodynamic balancing can have on the energy performance of the HDH system. First, we attempt to design a completely reversible HDH system. Then, we use this as a basis to investigate the effect of having finite-sized systems, of balancing the humidifier versus the dehumidifier, and of the number of extractions.

The performance parameter of interest in this study (and, generally, in thermal desalination itself) is the gained-output-ratio (GOR). GOR is the ratio of the latent heat of evaporation of the water produced to the net heat input to the cycle. This parameter is, essentially, the effectiveness of water production, which is an index of the amount of the heat recovery affected in the system.

$$\mathrm{GOR} = \frac{\dot{m}_{pw} \cdot h_{fg}}{\dot{Q}_{in}} \tag{20}$$

Latent heat is calculated at the average partial pressure of water vapor (in the moist air mixture) in the dehumidifier.

Recovery ratio (RR) is another parameter of interest in this study. RR is the amount of water desalinated per unit amount of feed entering the system.

$$\mathrm{RR} = \frac{\dot{m}_{pw}}{\dot{m}_{w}} \tag{21}$$

4.1. Continuous extractions with "infinitely large" HME devices: the upper limit on HDH performance

In section 2, we explained in detail how the 'remanent' irreversiblity (defined by Bejan [21]) is brought down to zero and complete thermodynamic balancing is achieved in a HME device. We use the closed form expressions [Eqs. (13–18)] presented in Sec. 2.4 to design a completely reversible HDH system. To achieve this we need to consider an infinitely large dehumidifier and humidifier (with enthalpy pinch, $\Psi_{deh} = \Psi_{hum} = 0$ kJ/kg dry air).

Figure 11 illustrates the mass flow rate ratio and HCR profiles for a HDH system with

100% effective humidifier and dehumidifier and complete thermodynamic balancing in the dehumidifier. It may be observed that the water-to-air mass flow rate ratio has to be varied from 1 to 31 in a continuous manner to achieve a spatially constant HCR of unity in the dehumidifier. For the system with the extraction profile as shown in Fig. 11, and at a feed temperature (T_a) of 20°C, salinity of 35 g/kg and a top brine temperature (T_c) of 80°C, the GOR was found to be 109.7 and the RR was 7.6%. The total entropy produced per unit amount of water distilled in the system was minimized to 10^{-3} kJ/kg·K.

[Figure 11 about here.]

The GOR achievable in a completely reversible HDH cycle may be evaluated using the expression (Eq. 22) derived in a previous publication (see appendix of Narayan et al. [3]). For a feed temperature (T_a) of 20°C, a top brine temperature (T_c) of 80°C and a recovery ratio of 7.6%, the reversible GOR that can be achieved is 123.3.

$$\mathrm{GOR}_{rev} = \frac{h_{fg} \cdot \left(1 - \frac{T_a}{T_c}\right)}{\mathrm{RR} \cdot g_{pw} + (1 - \mathrm{RR}) \cdot g_d - g_a} \tag{22}$$

Thus, with complete thermodynamic balancing (infinite extractions and injections) and infinite system size, the performance of the HDH system is about 88% of the reversible limit. Complete reversiblity cannot be achieved because it is only possible to fully balance either the dehumidifier or the humidifier in a given system and not both in the same design[3] (in Sec. 4.4, we show that balancing either the dehumidifier or the humidifier yields similar results). Thus, we conclude that the upper limit for HDH performance is below the reversible limit for thermal desalination systems.

[3]Both the humidifier and dehumidifier can be balanced in the same design only if a way to modify the process path for the air is possible. For example, if we were able to tailor different enthalpy-temperature functions for the moist air line in the humidifier and dehumidifier by modifying the physics of these processes. However, this is very hard to realise in a real design and hence, in the current publication we make the reasonable assumption that both the process paths are along the saturation line (see sec. 4.3).

4.2. Effect of finite system size

In the preceding section, we investigated 'infinitely' large HDH systems. This, of course, is a theoretical exercise to understand the performance limit of the system. In a real system, the humidifier and the dehumidifier will have an enthalpy pinch greater than zero. For example, a five-stage bubble column dehumidifier described in previous publications [28] has a Ψ of 15 kJ/kg dry air.

Figure 12 illustrates the effect of having finite size humidifier and dehumidifier on the system performance. As may be observed, the GOR values drop off rapidly as the enthalpy pinch increases. For example, when the enthalpy pinch is around 15 kJ/kg in the dehumidifier and the humidifier, the GOR is about 5 with infinite extractions. This is a large reduction from the GOR of 109.7 for the $\Psi = 0$ case. It leads us to conclude that thermodynamic balancing works best in systems with low enthalpy pinches in the dehumidifier and the humidifier. Further evidence corroborating this conclusion is described in Sec. 4.5.

[Figure 12 about here.]

4.3. Uncertainty associated with 'saturated air' approximation

Figure 12 also helps us quantify the uncertainity associated with assuming the process path for air to be along the saturation line. Thiel & Lienhard [14] performed boundary layer analysis on a dehumidifier and found that (based on the mass-averaged and energy-averaged definition of the 'bulk' state) the air follows a path different from the saturation curve (with a maximum deviation of about 10% in terms of the humidity ratio and the enthalpy associated with the terminal and the intermediate states in the process path). From Fig. 12, it may be observed that the propagated uncertainty in the GOR value due to the aforementioned deviation from the saturation line approximation is small. The uncertainty is less than 1% at Ψ values close to zero and reaches a maximum uncertainty of 11% at a Ψ of 27 kJ/kg of dry air (Ψ values greater than 27 kJ/kg are not of interest in this publication because of reasons stated later in this section). It is important to note that at $\Psi = 27$ kJ/kg of dry air, a 11% variation corresponds to an uncertainty of only 0.3 in terms of the GOR value.

4.4. Comparison of dehumidifier balanced and humidifier balanced systems

In Fig. 9, we illustrated the temperature profiles for two HDH systems: one with a balanced dehumidifier and the other with a balanced humidifier. In this section, we compare the performance of these two systems at various values of enthalpy pinch. As may be observed from Fig. 13, the performance is fairly similar. At lower values of enthalpy pinch ($\Psi < 7$ kJ/kg dry air) the dehumidifier balanced system has a slightly higher performance and at higher values of enthalpy pinch the humidifier balanced system is marginally better.

[Figure 13 about here.]

To understand the similar GOR values for the two systems studied in this section, let us consider Fig. 14. The entropy generated in the humidifier and the dehumidifier per kilogram of water desalinated in the system is illustrated for a fixed top brine temperature, feed water temperature and enthalpy pinches in the humidifier and the dehumidifier. When we completely balance the dehumidifier for this system, we reduce the entropy generated in the dehumidifier to a quarter of that in a system without mass extractions and injections. However, the entropy generated in the humidifier is increased by 65%. While we are balancing the dehumidifier, the humidifier is moving away from the balanced state. In the system with a completely balanced humidifier, the entropy generation in the humidifier is reduced to less than a third of that in a system without mass extractions or injections. The entropy generated in the dehumidifier changes little. The total entropy generated in the system per kg of water desalinated is about the same for both the system discussed here and hence these systems have a similar GOR value. We have observed a similar trend for other boundary conditions too.

[Figure 14 about here.]

In conclusion, based on studying the changes in entropy generated due to balancing in the various cases reported in this section, it was found that the reduction in total system

entropy generation due to continuous balancing is very similar at the same enthalpy pinches for the 'dehumidifier balanced' and the 'humidifier balanced' systems. Hence, the GOR was also found to be similar.

4.5. Effect of number of extractions

The effect of the number of extractions (at various enthalpy pinches) on the performance of the HDH system is shown in Fig. 15. Several important observations can be made from this chart.

First, it may be observed that thermodynamic balancing is effective in HDH cycles only when the humidifier and the dehumidifier have an enthalpy pinch less than about 27 kJ/kg dry air. For various boundary conditions it has been found that beyond the aforementioned value of enthalpy pinch the difference in performance (GOR) with that of a system without any extractions or injections is small (less than 20%). Further, at very low values of the enthalpy pinch ($\Psi \leq 7$ kJ/kg dry air) in the humidifier and the dehumidifier, continuous balancing with infinite number of extractions and injections was found to give much better results than that with a single extraction and injection. For the top brine temperature of 80°C, a feed water temperature of 20°C and 'infinitely' large humidifier and dehumidifier ($\Psi_{hum} = \Psi_{deh} = 0$ kJ/kg dry air), the GOR was found to be 8.2 for a single extraction (compared to a GOR of 109.7 for a similar system with infinite extractions). At higher values of enthalpy pinch ($7 < \Psi \leq 15$), a single extraction reduced the entropy generation of the total system roughly by a similar amount as an infinite number of extractions. At even higher values of enthalpy pinch ($15 < \Psi \leq 27$), a single extraction outperforms infinite extractions. This is a very suprising result. We try to understand this by looking at how the infinite and single extraction balancing affect the entropy generation in the humidifier and dehumidifier (see Fig. 16).

[Figure 15 about here.]

Figure 16 illustrates the entropy generated in the humidifier and the dehumidifier in

systems with zero, one and infinite extractions/injections at component enthalpy pinches of 20 kJ/kg dry air. It may be observed that when continuous extractions are applied, the entropy generated in the balanced component (the dehumidifier) is reduced but the entropy generated in the humidifier is increased. In other words, the humidifier is 'de-balanced' as the dehumidifier is balanced. For the single extractions case, even though the entropy generated in dehumidifier is reduced by a smaller amount than that in the infinite extractions case, the humidifier is not de-balanced. Thus, the total entropy generated is lower in the single extraction case and the GOR is higher.

[Figure 16 about here.]

Further, it is also noted here that it is possible to design a system with continuous extraction which neither balances the humidifier or the dehumidifier fully but balances both partially. Such a system is likely to have a higher performance than single extraction system. However, this is beyond the scope of the current publication.

5. Concluding Remarks

In the first half of this paper, a detailed study of thermodynamic balancing in HME devices is carried out. The following is a summary of the main conclusions of that study.

1. A novel "enthalpy pinch" has been defined for combined heat and mass exchange devices analogous to the temperature pinch traditionally defined for heat exchangers. Enthalpy pinch (Ψ) combines stream-to-stream temperature and humidity ratio differences, and is directly related to the effectiveness of the device. We recommend it for use in thermodynamic analyses of systems containing HME devices.
2. Closed form equations for the temperature and humidity ratio profiles of a completely and continuously balanced HME device with zero 'remanent' irreversiblity is presented in this paper for the first time in literature.

3. It is observed that this state of complete thermodynamic balancing (in humidifiers and dehumidifiers) is closer to a state of constant local humidity ratio difference than to that of a constant stream-to-stream temperature difference.
4. By continuous extraction of mass in a dehumidifier, the entropy generation in the device can be brought down to $\frac{1}{4}^{\text{th}}$ of that in a device without extractions. By a single extraction it can be brought down to $\frac{3}{5}^{\text{rd}}$. Either water or air may be extracted from the humidifier in these cases.

Further, these observations were used in the second part of the paper for the design of thermodynamically balanced HDH systems, and the following are the salient features of that part of the study.

1. Detailed algorithms for design of HDH systems with mass extractions and injections using the temperature versus enthalpy diagram have been developed in this paper. These were developed for both continuous and discrete extractions and injections.
2. An *almost* completely reversible HDH system was designed using an "infinitely large" humidifier and dehumidifier with continuous mass extraction and injection. A theoretical gained-output-ratio of 109.7 approaching the reversible limit of 123.3 was evaluated for this ideal system with the total entropy generation approaching zero ($\frac{\dot{S}_{gen}}{\dot{m}_{pw}} \approx 10^{-3}$ kJ/K· kg water produced).
3. The uncertainty of the final results reported in the paper associated with the approximation of the air being saturated at all points in the humidification and dehumidification processes was evaluated to be reasonably small based on the boundary layer data from Thiel and Lienhard [14].
4. It is found that the performance of an HDH system with a completely balanced humidifier and that with a completely balanced dehumidifier are similar. This is explained by examining the entropy generated in each component in the system in each case.
5. It is found that thermodynamic balancing is effective in HDH only when the HME devices have an appropriately low enthalpy pinch ($\Psi \leq 27$ kJ/kg dry air).

6. At very low values of the enthalpy pinch ($\Psi \leq 7$ kJ/kg dry air) in the humidifier and the dehumidifier, continuous balancing with an infinite number of extractions and injections was found to give much better results than that with a single extraction and injection. At higher values of enthalpy pinch ($7 < \Psi \leq 15$), a single extraction reduced the entropy generation of the total system by a similar amount as infinite extractions. At even higher values of enthalpy pinch ($15 < \Psi \leq 27$), single extraction outperformed infinite extractions and at $\Psi > 27$, thermodynamic balancing has no significant effect on the performance of the HDH system.

Acknowledgments

The authors would like to thank the King Fahd University of Petroleum and Minerals for funding the research reported in this paper through the Center for Clean Water and Clean Energy at MIT and KFUPM (project # R4-CW-08). The second author (RKM) would like to acknowledge financial support provided by the International Fulbright Science & Technology Award, U.S. Department of State.

References

[1] G. P. Narayan, M. H. Sharqawy, E. K. Summers, J. H. Lienhard V, S. M. Zubair, and M. A. Antar, "The potential of solar-driven humidification-dehumidification desalination for small-scale decentralized water production," *Renewable and Sustainable Energy Reviews*, vol. 14, pp. 1187–1201, 2010.

[2] K. Bourouni, M. Chaibi, and L. Tadrist, "Water desalination by humidification and dehumidification of air: state of the art," *Desalination*, vol. 137, p. 167176, 2001.

[3] G. P. Narayan, M. H. Sharqawy, J. H. Lienhard V, and S. M. Zubair, "Thermodynamic analysis of humidification dehumidification desalination cycles," *Desalination and Water Treatment*, vol. 16, pp. 339–353, 2010.

[4] K. H. Mistry, A. Mitsos, and J. H. Lienhard V, "Optimal operating conditions and configurations for humidification-dehumidification desalination cycles," *International Journal of Thermal Sciences*, vol. 50, pp. 779–789, 2011.

[5] J. A. Miller, "Numerical balancing in a humdification dehumidification desalination system," Master's thesis, Massachusetts Institute of Technology, 2011.

[6] G. P. Narayan, J. H. Lienhard V, and S. M. Zubair, "Entropy generation minimization of combined heat and mass transfer devices," *International Journal of Thermal Sciences*, vol. 49, pp. 2057–66, 2010.

[7] H. Müller-Holst, *Solar thermal desalination using the Multiple Effect Humidification (MEH) method in Solar Desalination for the 21st Century*, ch. 15, pp. 215–25. NATO Security through Science Series, Springer, Dordrecht, 2007.

[8] H. Müller-Holst, *Mehrfacheffekt-Feuchtluftdestillation bei Umgebungsdruck - Verfahrensoptimierung und Anwendungen*. PhD thesis, Technische Universität Berlin, 2002.

[9] M. Zamen, S. M. Soufari, and M. Amidpour, "Improvement of solar humdification-dehumidification desalination using multi-stage process," *Chemical Engineering Transactions*, vol. 25, pp. 1091–1096, 2011.

[10] T. Schlickum, "Device for separating a liquid from its dissolved matters." European Patent, EP 1770068 A2. 2007.

[11] S. Hou, "Two-stage solar multi-effect humidification dehumidification desalination process plotted from pinch analysis," *Desalination*, vol. 222, p. 5728, 2008.

[12] T. Brendel, *Solare Meewasserental sungsanlagen mit mehrstufiger verdungtung.* PhD thesis, Ruhr University Bochum, 2003.

[13] T. Brendel, "Process to distil and desalinate water in contra-flow evaporation humidifier unit with progressive removal of evaporated fluid," 2003. German Patent #DE10215079 (A1).

[14] G. P. Thiel and J. H. Lienhard V, "Entropy generation in condensation in the presence of high concentrations of noncondensable gases," *International Journal of Heat and Mass Transfer*, vol. 55, pp. 5133–5147, May 2012.

[15] M. A. Younis, M. A. Darwish, and F. Juwayhel, "Experimental and theoretical study of a humidification-dehumidification desalting system," *Desalination*, vol. 94, pp. 11–24, 1993.

[16] R. K. McGovern, G. P. Thiel, G. P. Narayan, S. M. Zubair, and J. H. Lienhard V, "Evaluation of the performance limits of humidification dehumidification desalination systems via a saturation curve analysis," *Applied Energy*, 2012. In Press. DOI link: http://dx.doi.org/10.1016/j.apenergy.2012.06.025.

[17] W. Grune, T. Thompson, and R. Collins, "New applications of thermodynamic principles to solar distillation," in *Meeting of the American Society of Mechanical Engineers*, no. Paper 61-5A-45, New York, 1961.

[18] G. P. Narayan, K. H. Mistry, M. H. Sharqawy, S. M. Zubair, and J. H. Lienhard V, "Energy effectiveness of simultaneous heat and mass exchange devices," *Frontiers in Heat and Mass Transfer*, vol. 1, pp. 1–13, 2010.

[19] G. P. Narayan, R. K. McGovern, S. M. Zubair, and J. H. Lienhard V, "Variable pressure humidification dehumidification desalination," in *Proceedings of ASME/JSME 8th Thermal Engineering Joint conference, Hawaii*, March 13-17 2011.

[20] G. P. Narayan, R. K. McGovern, S. M. Zubair, and J. H. Lienhard V, "High-temperature steam-driven varied-pressure humidification-dehumidification system coupled with reverse osmosis for energy-efficient seawater desalination," *Energy*, vol. 37, pp. 482–93, 2012.

[21] A. Bejan, *Entropy generation minimization: the method of thermodynamic optimization of finite size systems and finite time processes.* Boca Raton, FL: CRC Press, 1996.

[22] R. K. Shah and D. P. Sekulić, *Fundamentals of heat exchanger design.* John Wiley and Sons, 2003.

[23] M. H. Sharqawy, J. H. L. V, and S. M. Zubair, "Thermophysical properties of seawater: A review of existing correlations and data," *Desalination and Water Treatment*, vol. 16, pp. 354–80, 2010.

[24] S. Pruss and W. Wagner, "The iapws formulation 1995 for the thermodynamic properties of ordinary water substance for general and scientific use," *Journal of Physical and Chemical Reference Data*, vol. 31, pp. 387–535, 2002.

[25] R. W. Hyland and A. Wexler, "Formulations for the Thermodynamic Properties of Dry Air from 173.15 K to 473.15 K, and of Saturated Moist Air From 173.15 K to 372.15 K, at Pressures to 5 MPa," *ASHRAE Transactions*, vol. Part 2A (RP-216), no. 2794, pp. 520–535, 1983b.

[26] D. J. Wessel, *ASHRAE Fundamentals Handbook 2001 (SI Edition).* American Society of Heating, Refrigerating, and Air-Conditioning Engineers, 2001.

[27] E. W. Lemmon, M. L. Huber, and M. O. McLinden, "Standard reference database 23: Reference fluid thermodynamic and transport properties," tech. rep., NIST - REFPROP, Version 8.0 (2007).

[28] G. P. Narayan, *Thermal Design of Humidification Dehumidification Systems for Affordable Small-scale Desalination.* PhD thesis, Massachusetts Institute of Technology, 2012.

Appendices

A: Approximations involved in the thermodynamic analysis proposed in this paper

- In the temperature-enthalpy diagrams and associated calculations the enthalpy of both water and air is defined per unit amount of dry air (h^*). This makes graphical representation and application easier. Also, as a result of this modification, the slope of the water line in these diagrams is $\frac{1}{m_r \cdot c_{p,w}}$. This newly defined enthalpy represents control volume location along the fluid flow path in the HME device (the humidifier or dehumidifier). For representative purposes the enthalpy is non-dimensionalised by the total streamwise enthalpy change (Δh^*) and is presented as non-dimensional location in the current publication.

- Pure water is approximated to be produced at the feedwater temperature in the dehumidifier. The maximum error due to such an approximation is reasonably small ($< 2\%$) because the enthalpy of the pure water is very small compared that of the feedwater.

- Enthalpy and entropy data is input into Matlab from a discrete database. There is a small convergence error associated with the same. The discretization of the database was small enough such that this error was reasonably small ($<1\%$)

- Air follows a process path such that it is assumed to be at a 'bulk' state which is always on the saturation line. This approximation has been dealt with in great detail in a separate publication [16]. In the current publication, we have shown that the uncertainty associated with the aforementioned approximation is reasonably small (see Sec. 4.3).

B: Algorithms for modeling HDH systems with and without thermodynamic balancing

[Figure 17 about here.]

[Figure 18 about here.]

[Figure 19 about here.]

Contents

List of Figures

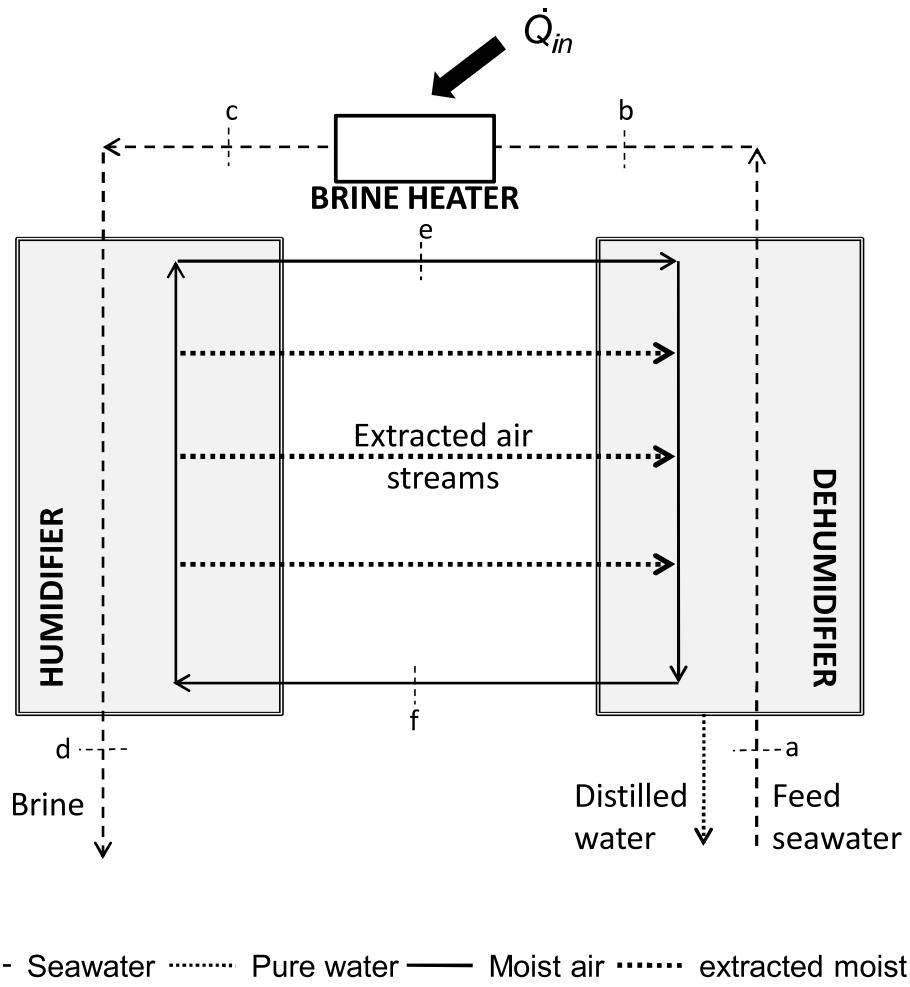

Figure 1: Schematic diagram of a water-heated, closed-air, open-water humidification-dehumidification desalination system with mass extraction and injection of the moist air stream.

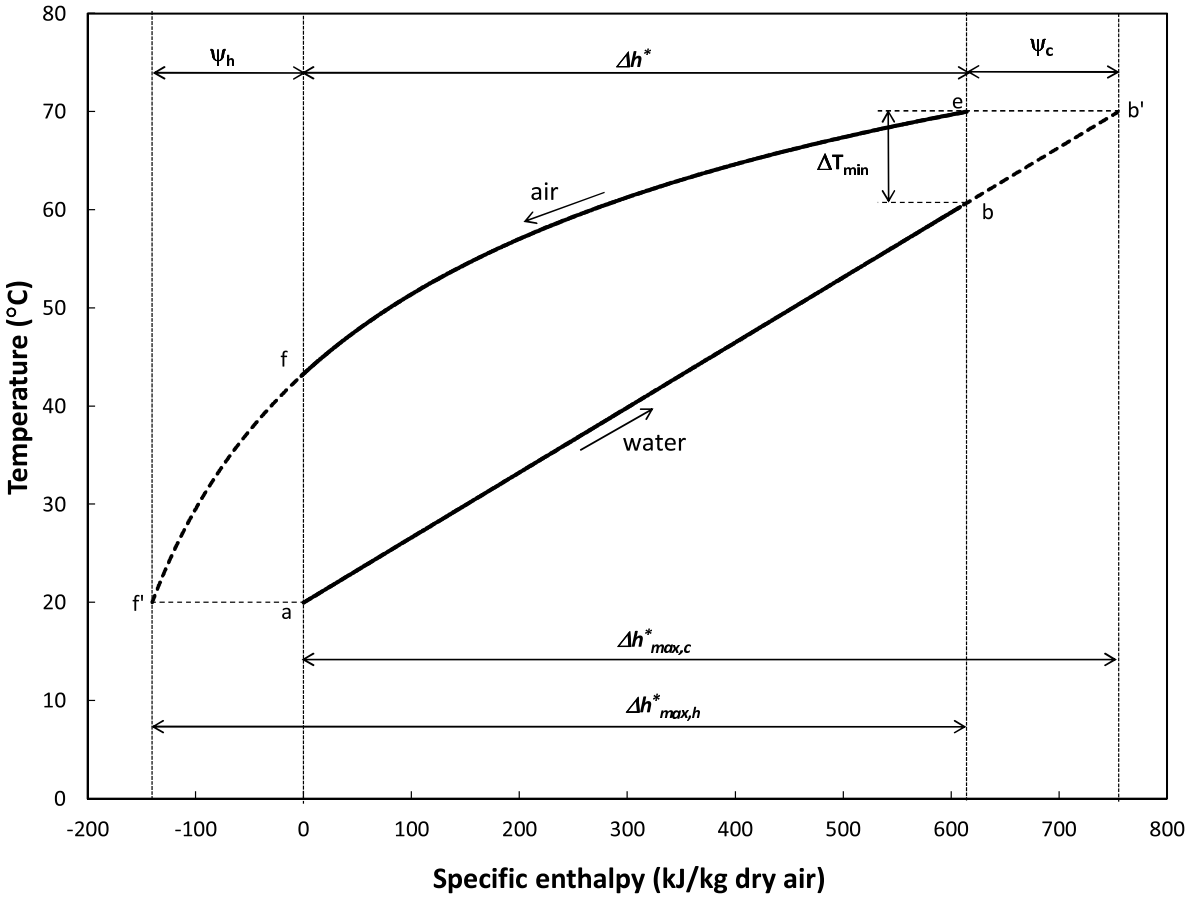

Figure 2: Temperature versus enthalpy diagram representing the dehumidification process highlighting the maximum change in enthalpy rates (per kg of dry air) that can be achieved by each of the fluid streams ($\Delta h_{max,c}$ and $\Delta h_{max,h}$) and the terminal enthalpy pinches (Ψ_c and Ψ_h).

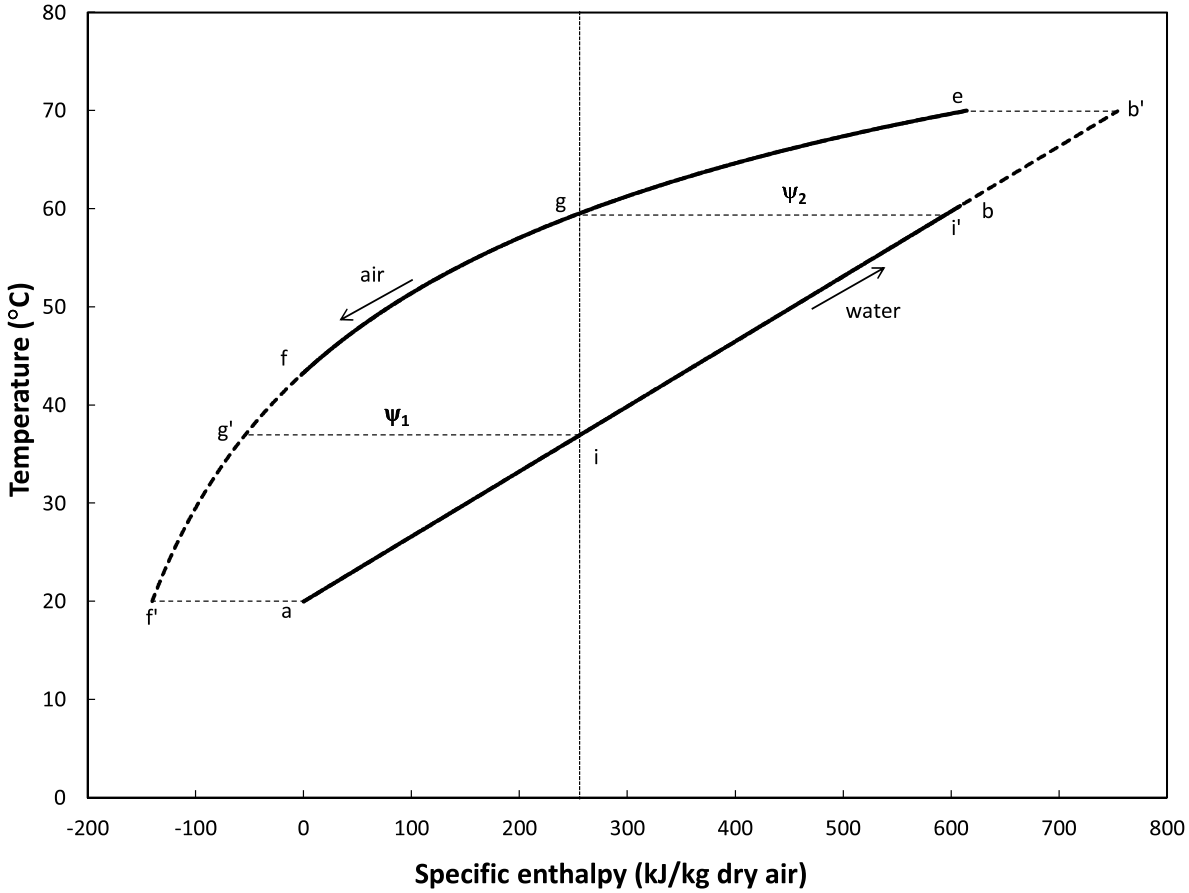

Figure 3: Temperature versus enthalpy diagram for the dehumidification process highlighting 'loss in ideal enthalpy' or enthalpy pinch at any given location (Ψ_{local}) as a measure of local effectiveness in HME devices.

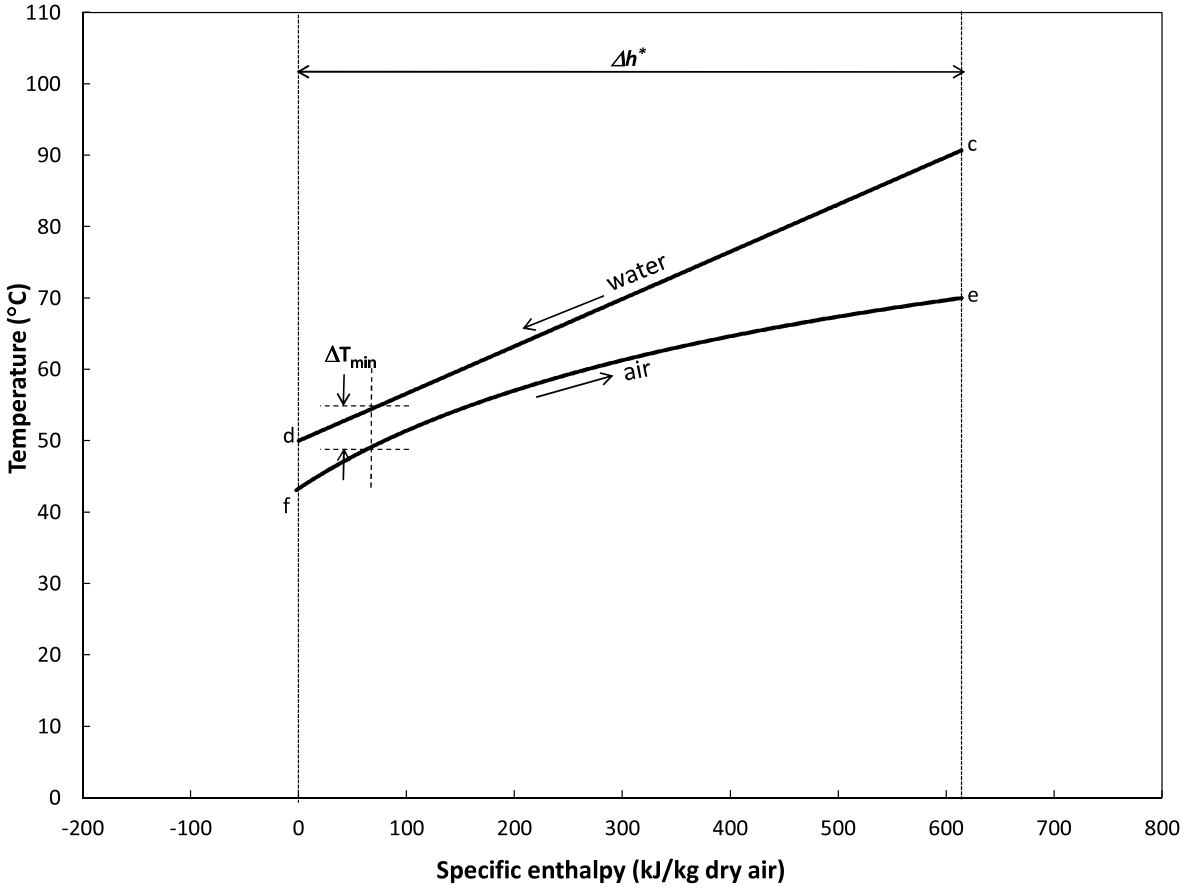

Figure 4: Temperature versus enthalpy diagram representing the humidification process highligting the 'pinch point' occuring at an intermediate location rather than at a terminal one.

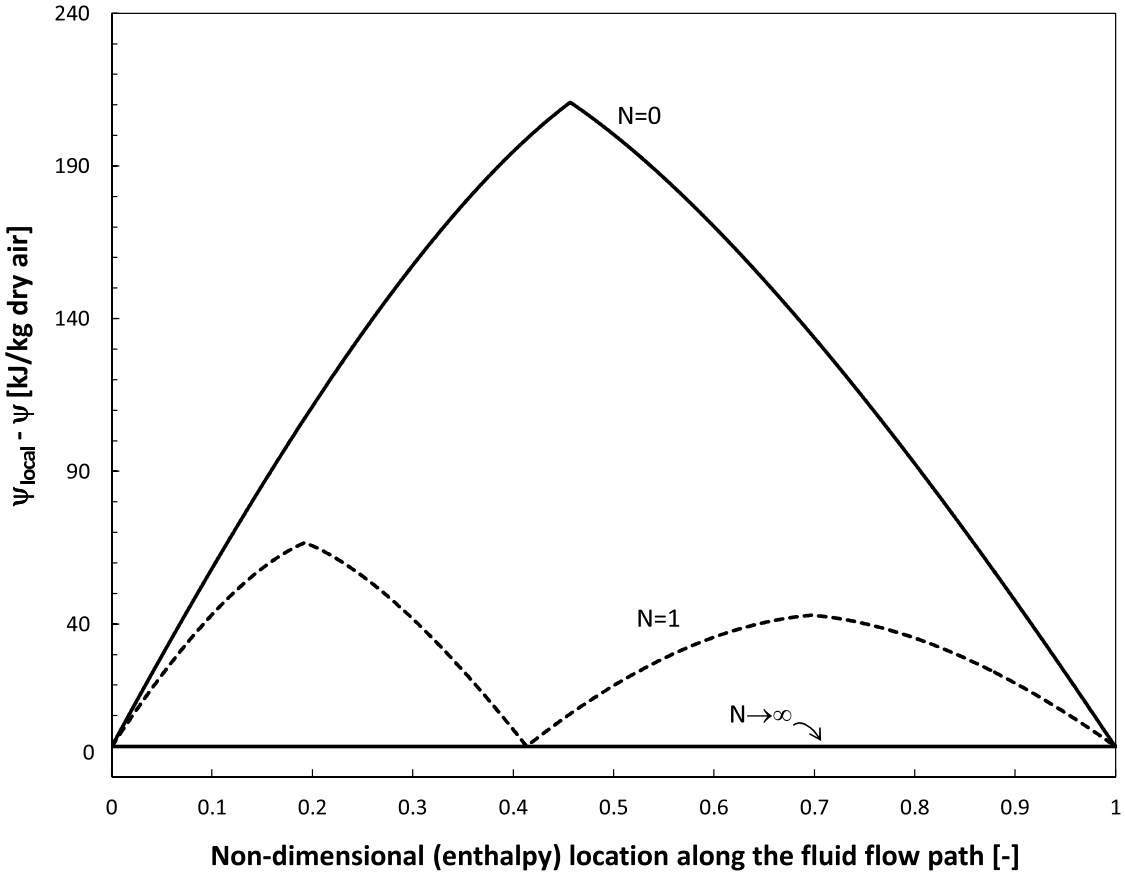

Figure 5: A plot of local enthalpy pinch values (Ψ_{local}) relative to the overall enthalpy pinch (Ψ) to illustrate the effect of extractions in a dehumidifier with the control volume balanced case.

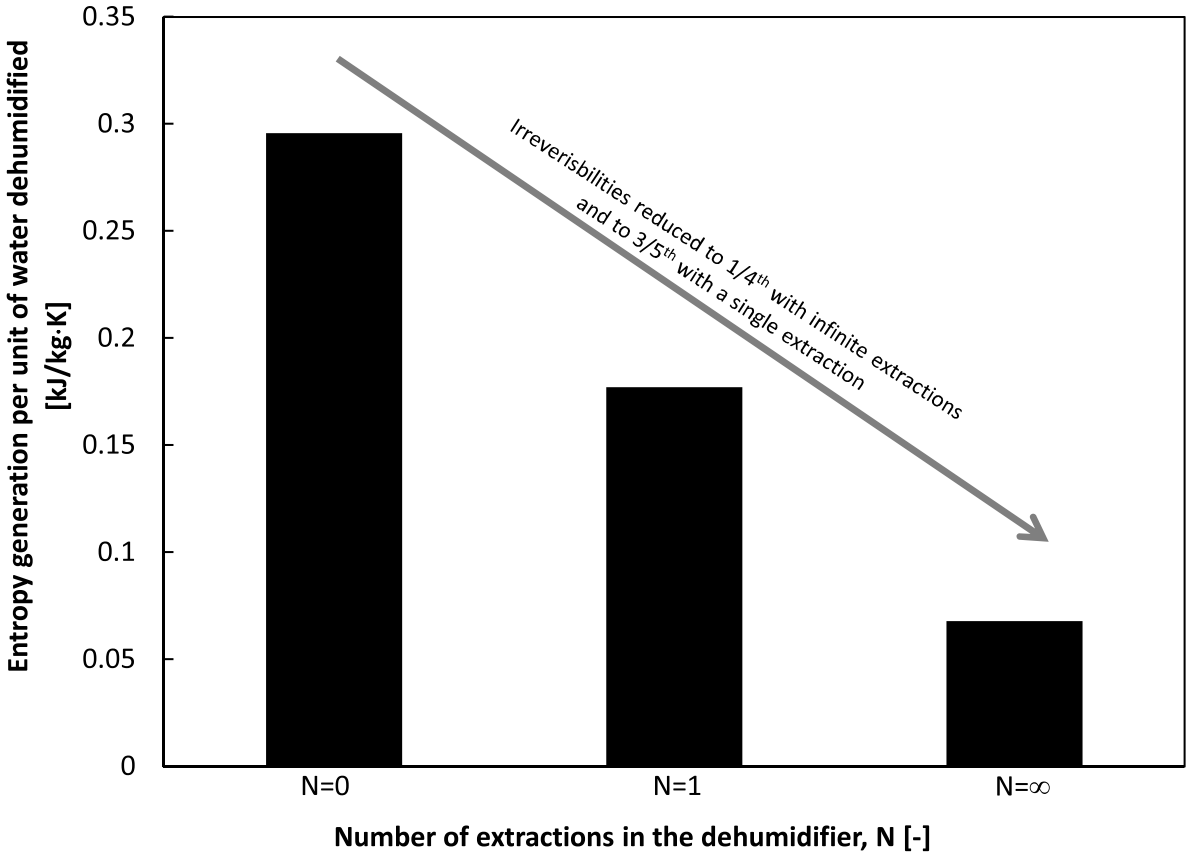

Figure 6: Effect of extraction on the irreversiblity in the dehumidifier evaluated at $T_a = 20°C$; $T_e = 70°C$; $\Psi_{deh} = 20$ kJ/kg dry air; HCR =1.

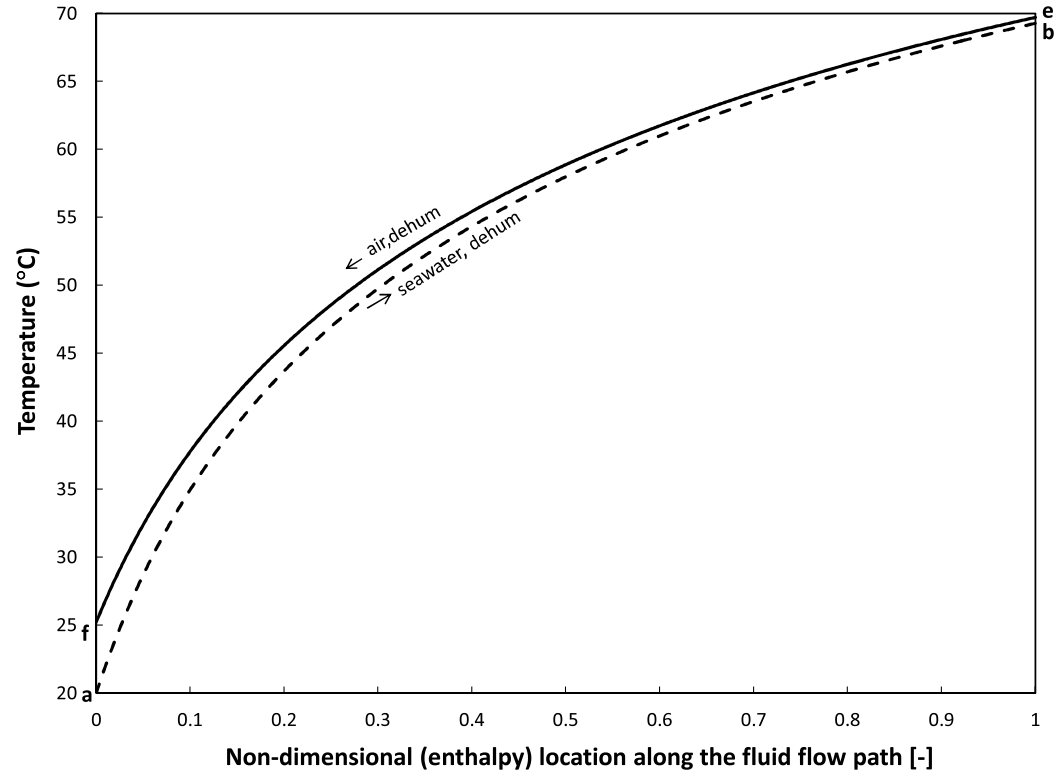

(a) Temperature profile

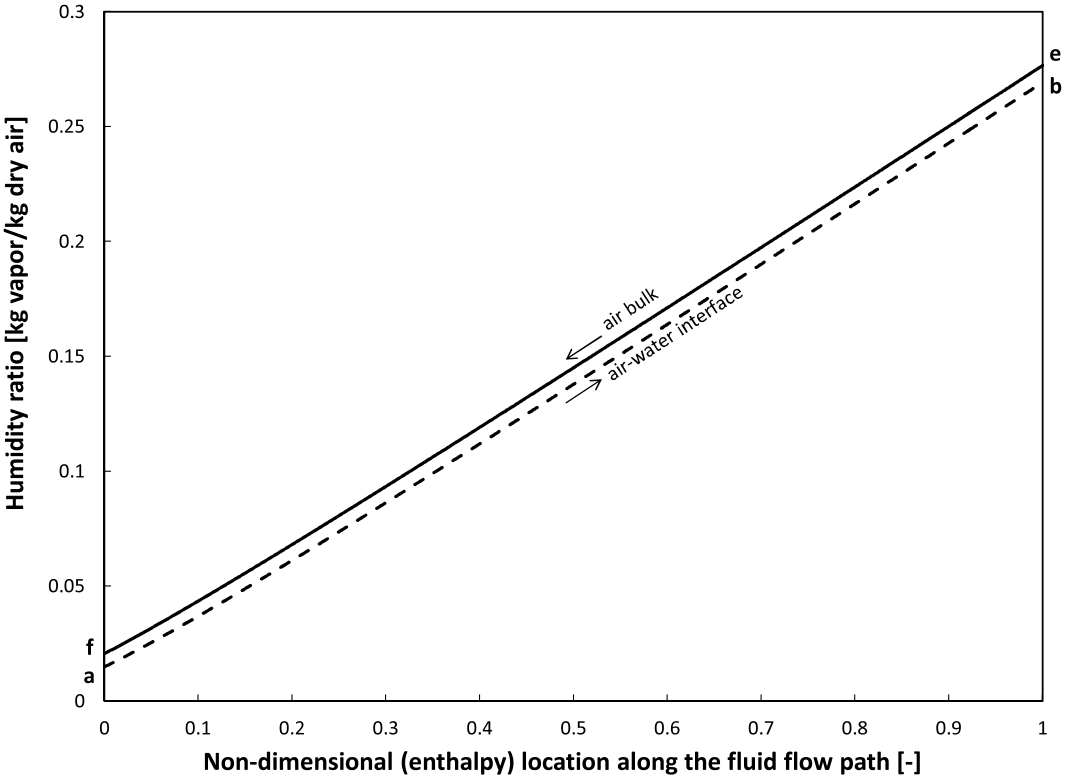

(b) Humidity ratio profile

Figure 7: An illustration of (a) temperature and (b) humidity ratio profiles in an dehumidifier with complete thermodynamic balancing by continuous extraction.

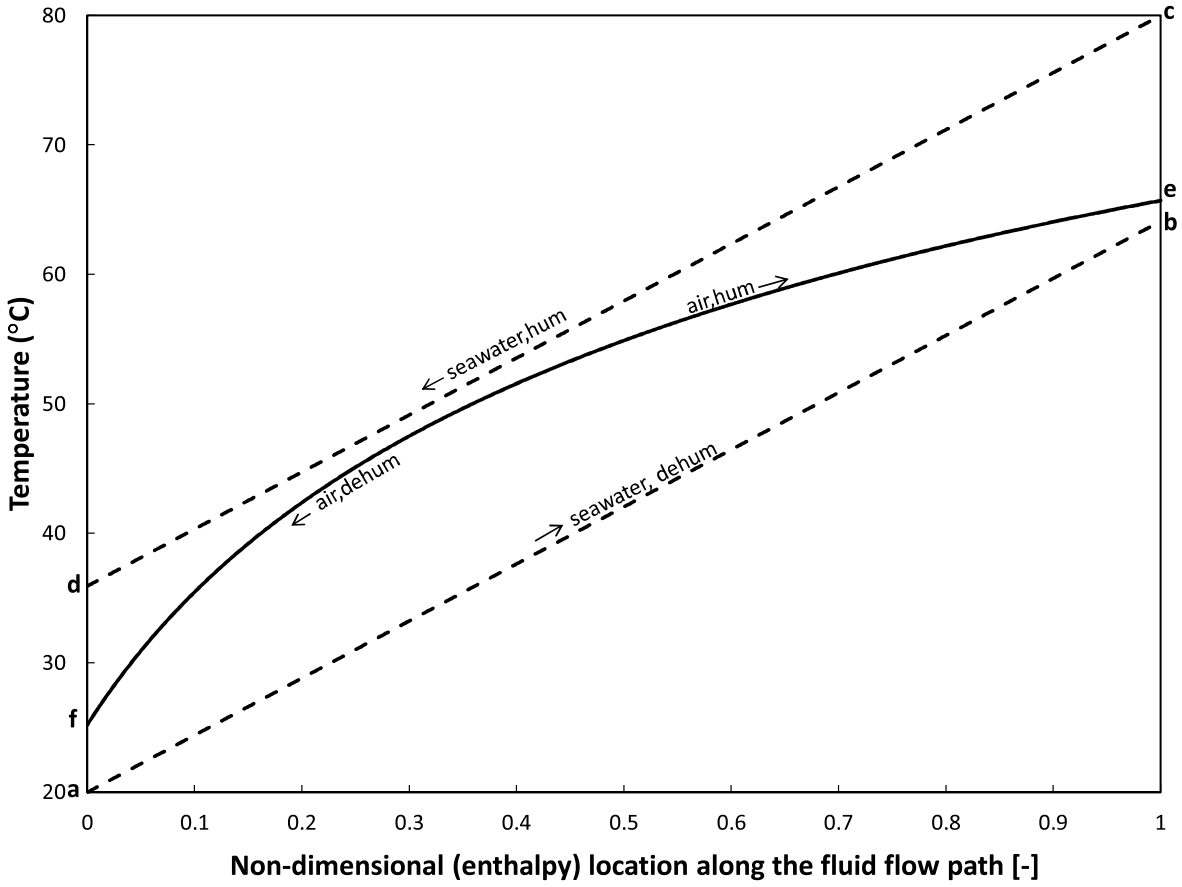

Figure 8: Temperature profile representing the HDH system without extractions or injections. Boundary conditions: $T_a = 20°\text{C}$; $T_c = 80°\text{C}$; $\Psi_{deh} = \Psi_{hum} = 20$ kJ/kg dry air.

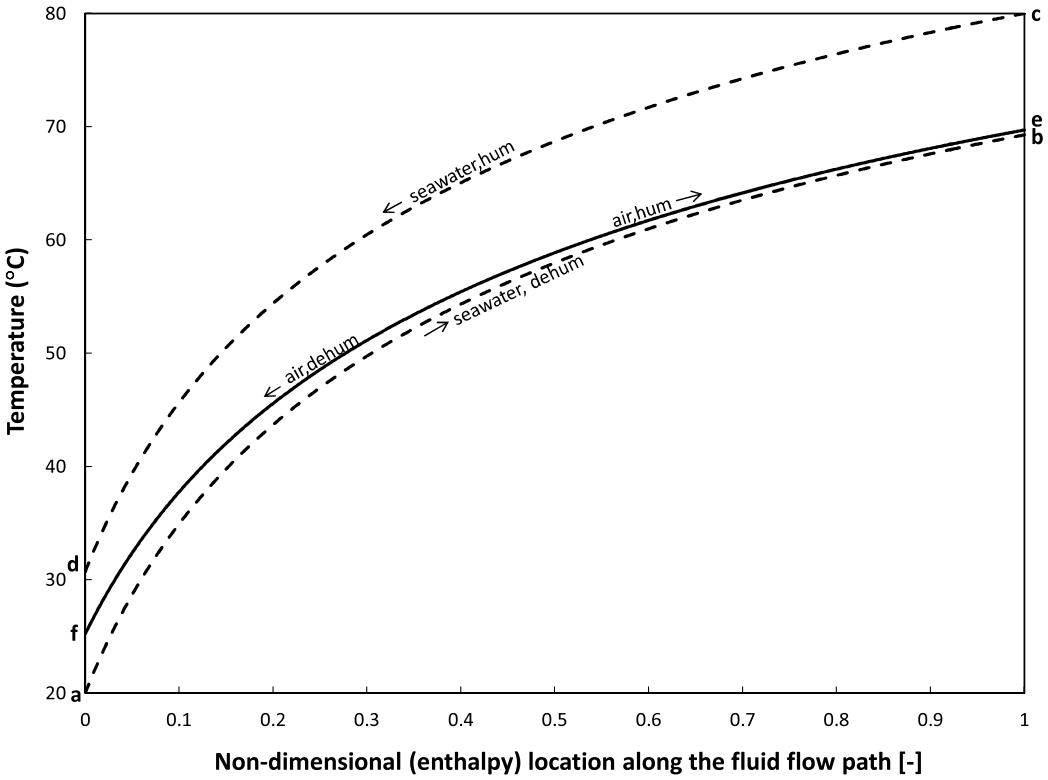

(a) Dehumidifier balanced

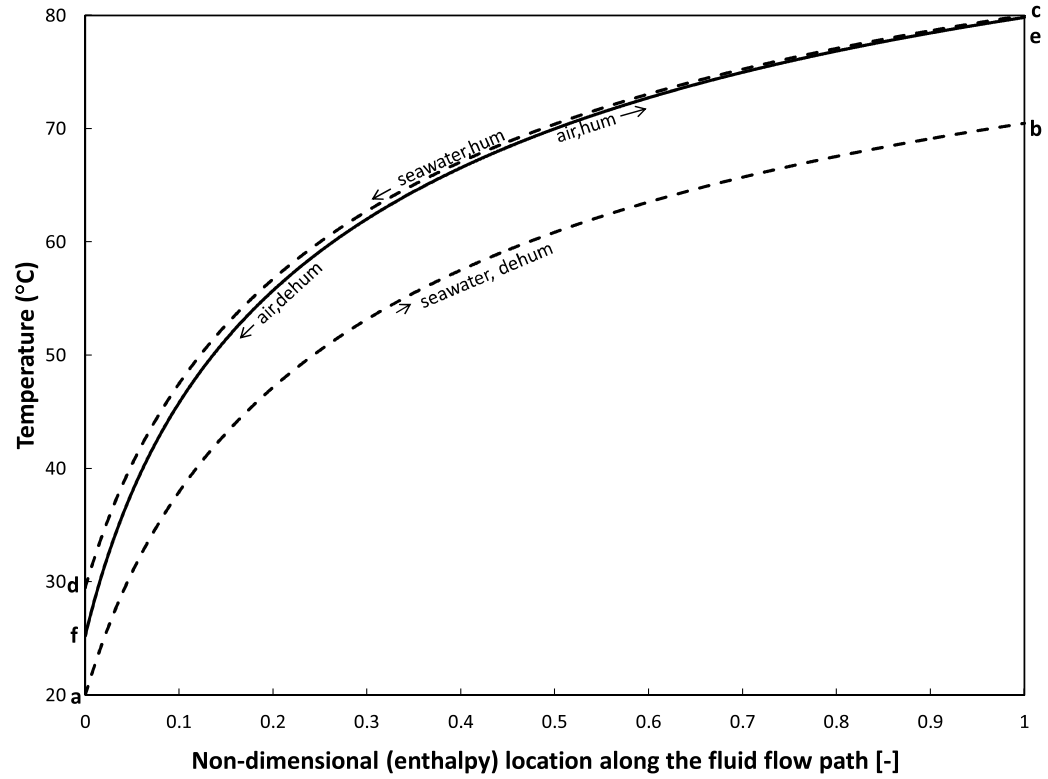

(b) Humidifier balanced

Figure 9: Temperature profiles representing the HDH system with continuous extractions to completely balance (a) dehumidifier and (b) humidifier. Boundary conditions: $T_a = 20°\text{C}$; $T_c = 80°\text{C}$; $\Psi_{deh} = \Psi_{hum} = 20$ kJ/kg dry air.

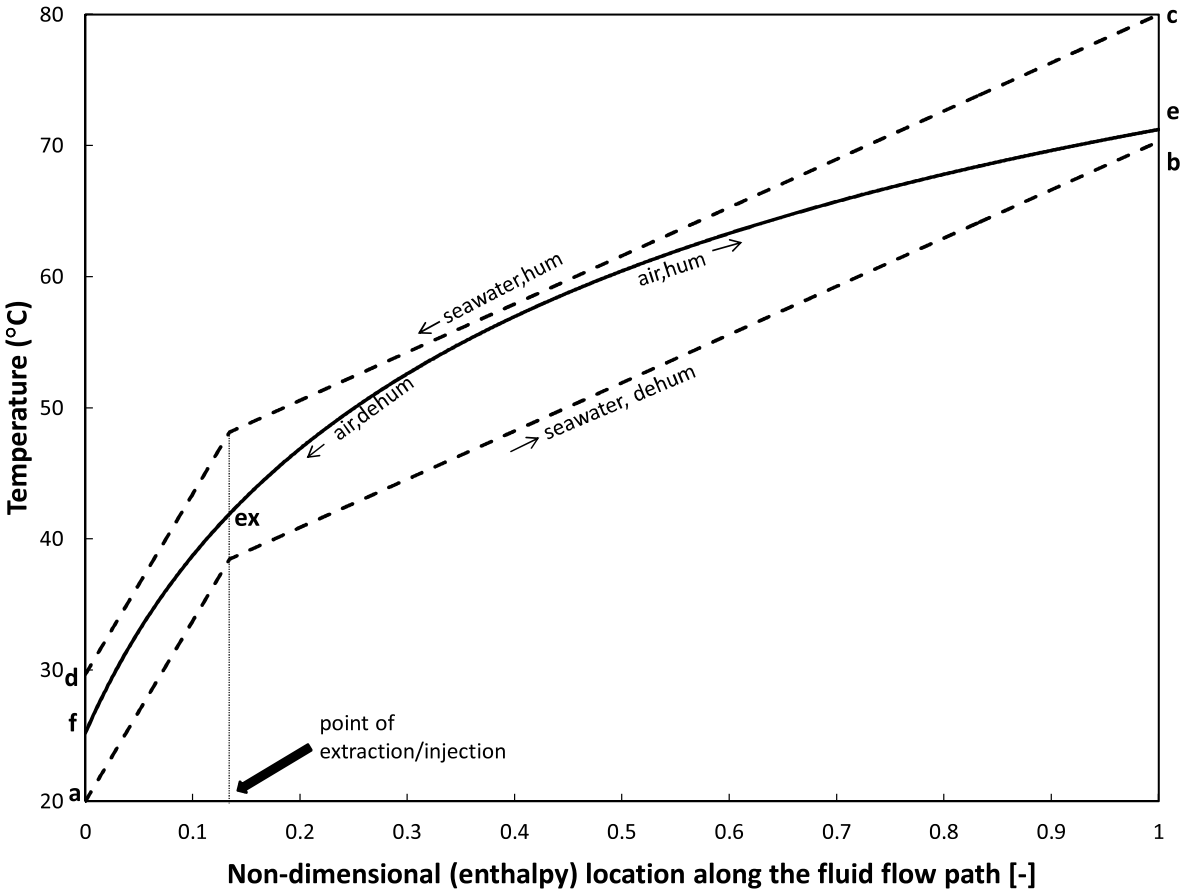

Figure 10: Temperature profile representing the HDH system with a single extraction. Boundary conditions: $T_a = 20°\text{C}$; $T_c = 80°\text{C}$; $\Psi_{deh} = \Psi_{hum} = 20$ kJ/kg dry air.

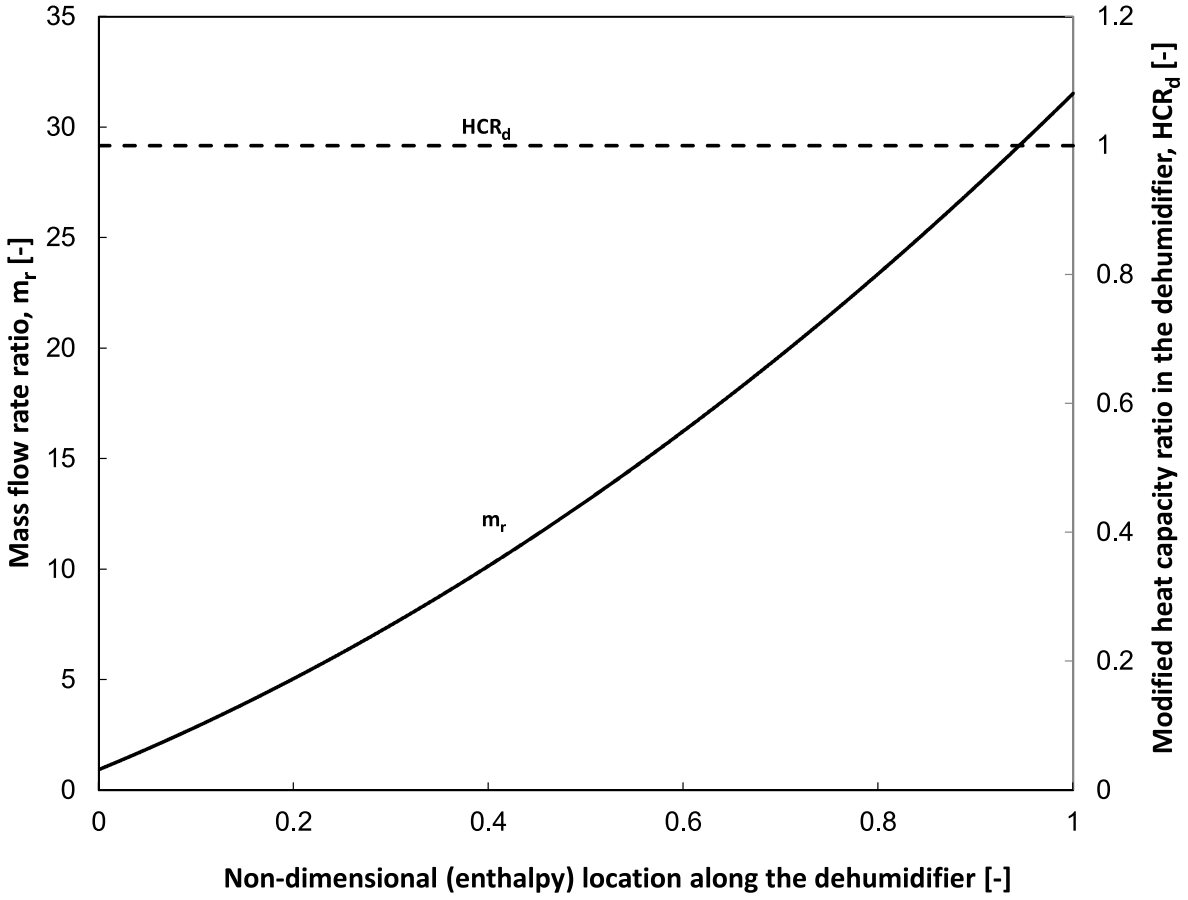

Figure 11: Mass flow rate ratio and HCR profile for complete thermodynamic balancing in a HDH system with 100% effective humidifier and dehumidifier. Boundary conditions: $T_a = 20°$C; $sal = 35$ g/kg; $T_c = 80°$C; $\Psi_{deh} = \Psi_{hum} = 0$ kJ/kg dry air; $N = \infty$; System performance: **GOR = 109.7; RR=7.6%.**

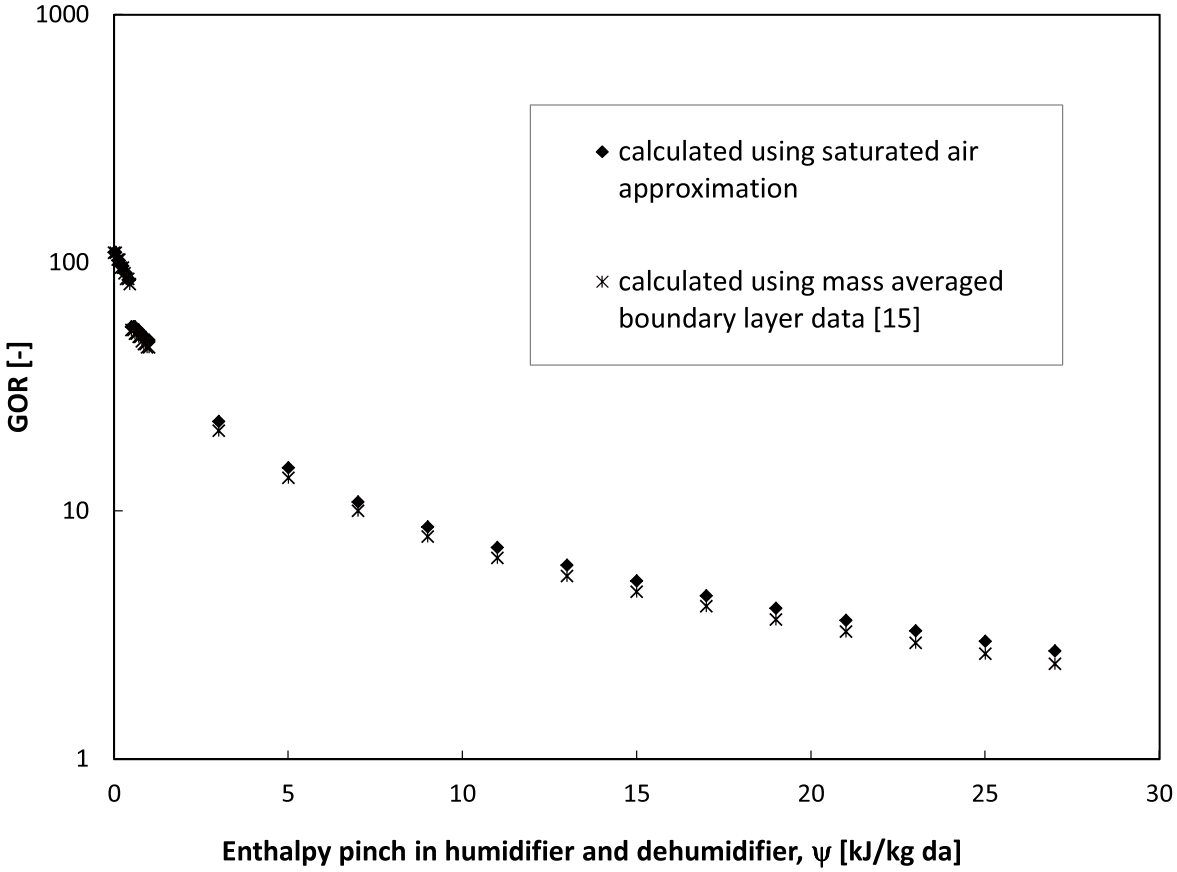

Figure 12: Effect of having finite-size HME devices on the performance of the HDH system with infinite extractions highlighting the maximum possible uncertainity associated with using the saturation line as the air process path. Boundary conditions: $T_a = 20°$C; $sal = 35$ g/kg; $T_c = 80°$C; $N = \infty$; HCR$_{deh}$=1.

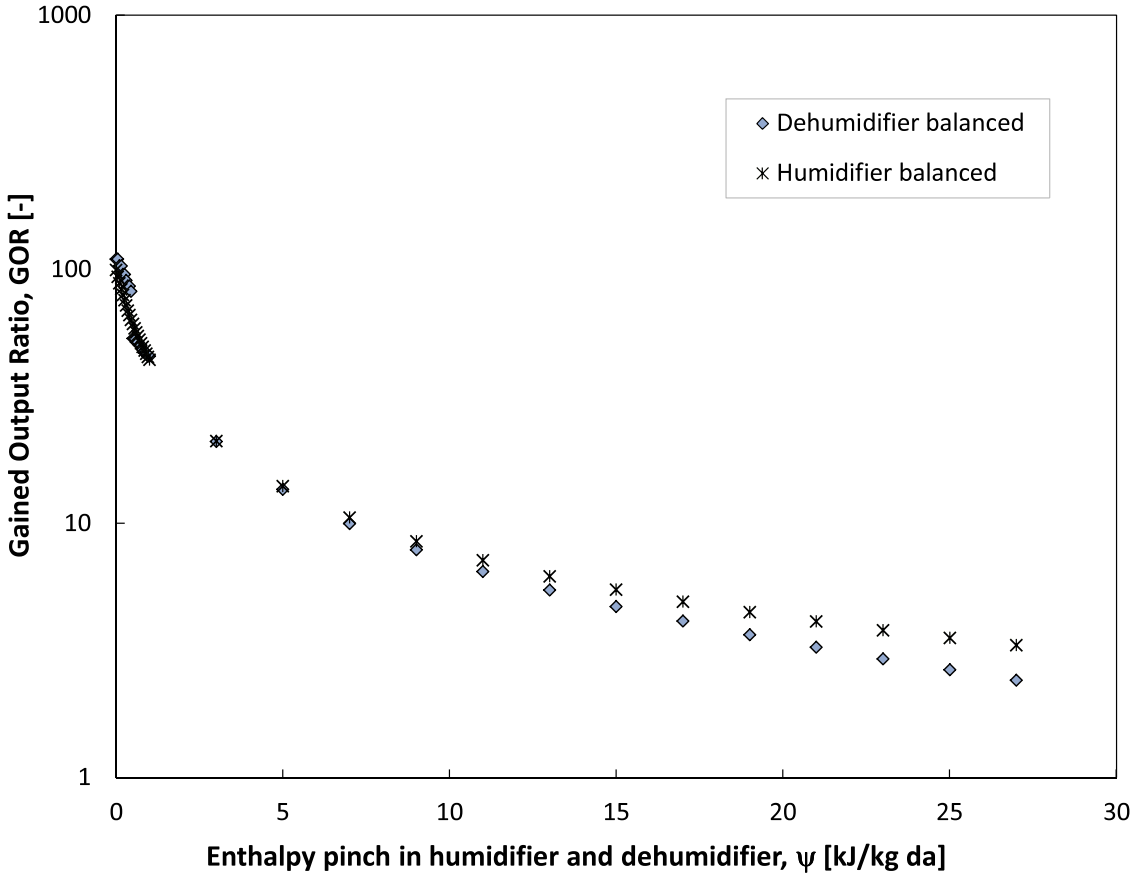

Figure 13: Comparison of performance of the HDH system with infinite extractions for complete thermodynamic balancing of humidifier with that for complete thermodynamic balancing of the dehumidifier. Boundary conditions: $T_a = 20°$C; $sal = 35$ g/kg; $T_c = 80°$C; $N = \infty$; HCR$_{deh}$=1.

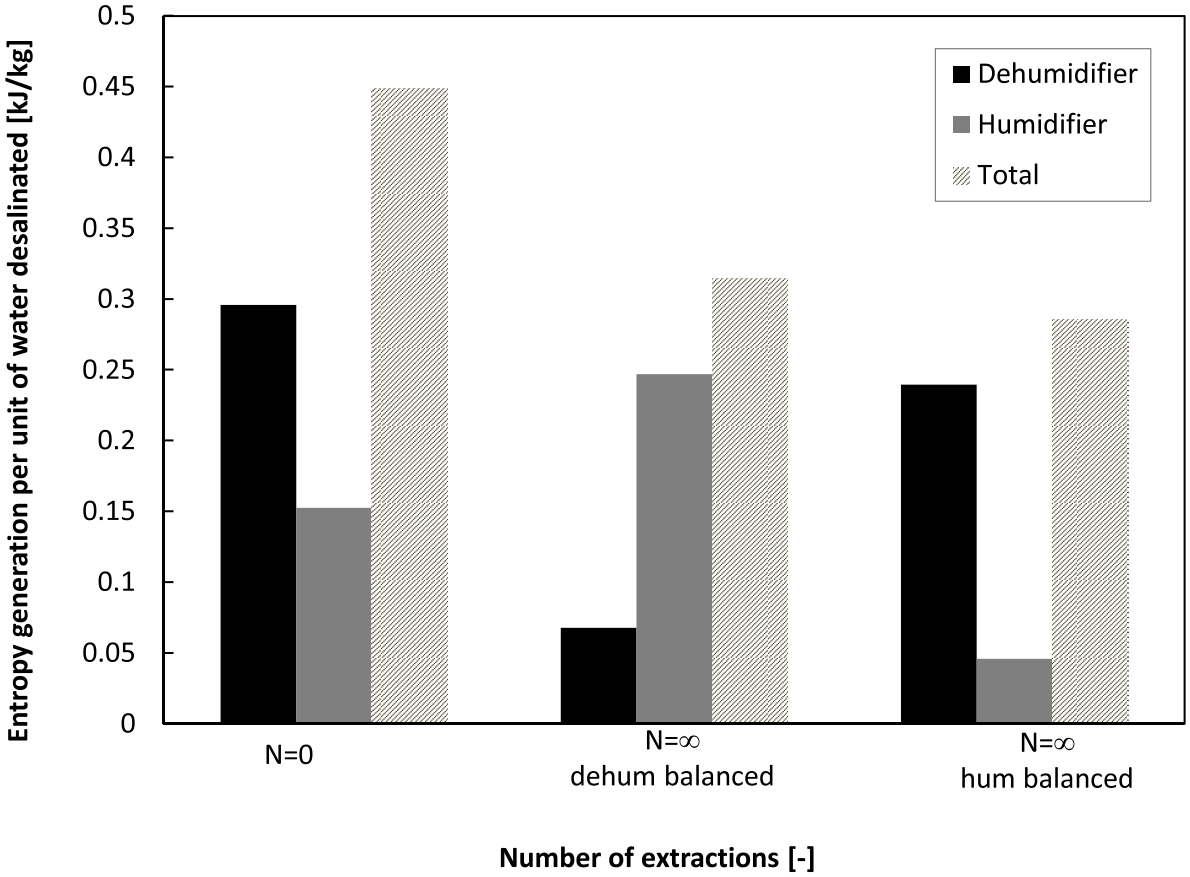

Figure 14: Reduction in total system irreverisibility with complete thermodynamic balancing of either the humidifier or the dehumidifier in HDH. Boundary conditions: T_a = 20°C; sal = 35 g/kg; T_c = 80°C; $\Psi_{deh} = \Psi_{hum} = 20$ kJ/kg dry air; HCR_{deh}=1 or ; HCR_{hum}=1.

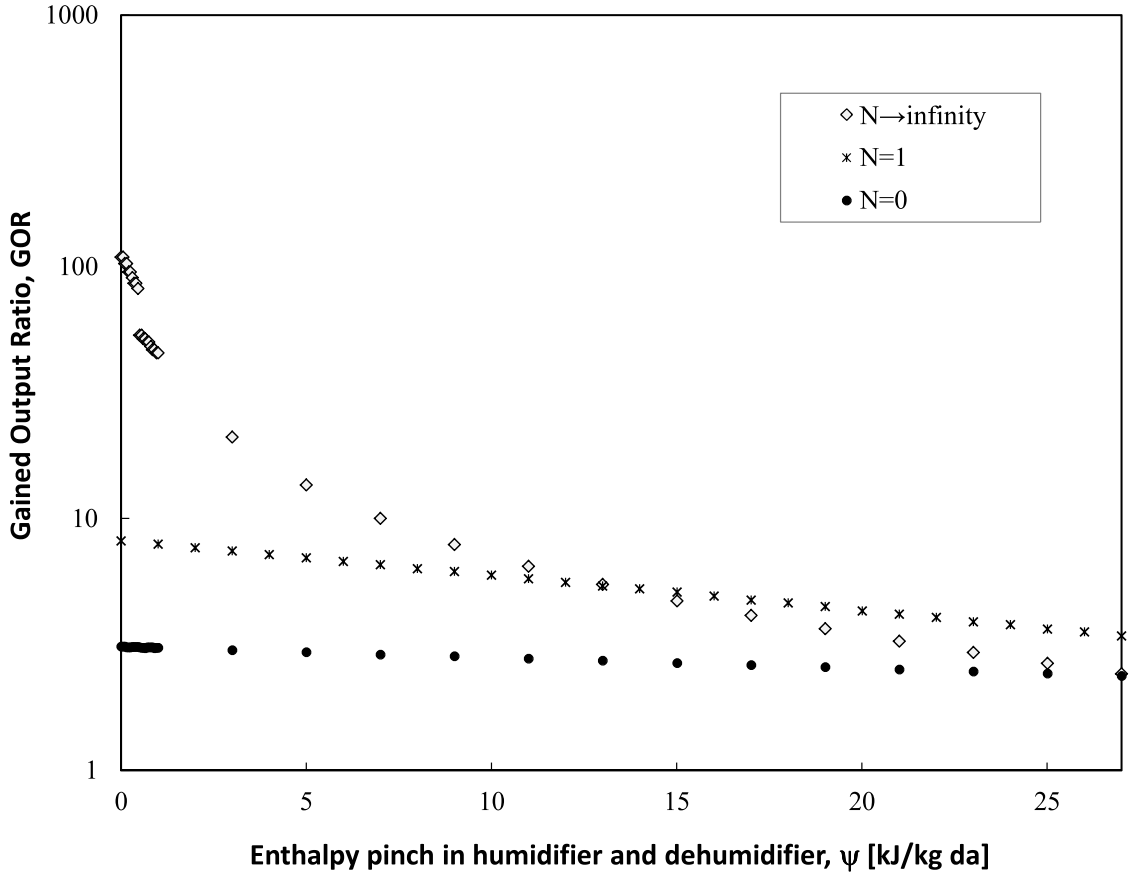

Figure 15: Effect of number of extractions (for thermodynamic balancing) on the performance of the HDH system with finite and infinite size HME devices. Boundary conditions: $T_a = 20°C$; $sal = 35$ g/kg; $T_c = 80°C$; HCR_{deh}=1.

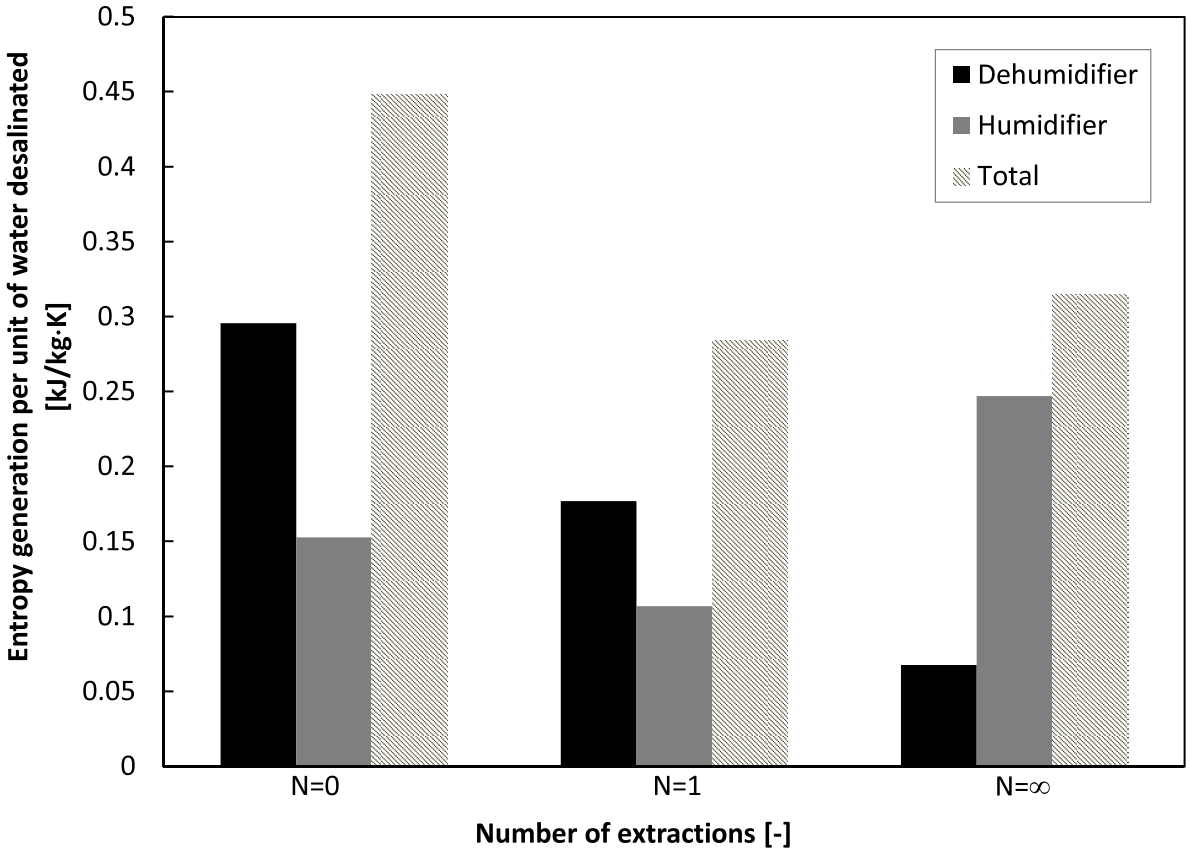

Figure 16: Effect of extraction on total system irreversiblities. Boundary conditions: $T_a = 20°C$; $sal = 35$ g/kg; $T_c = 80°C$; $\Psi_{deh} = \Psi_{hum} = 20$ kJ/kg dry air; HCR_{deh}=1.

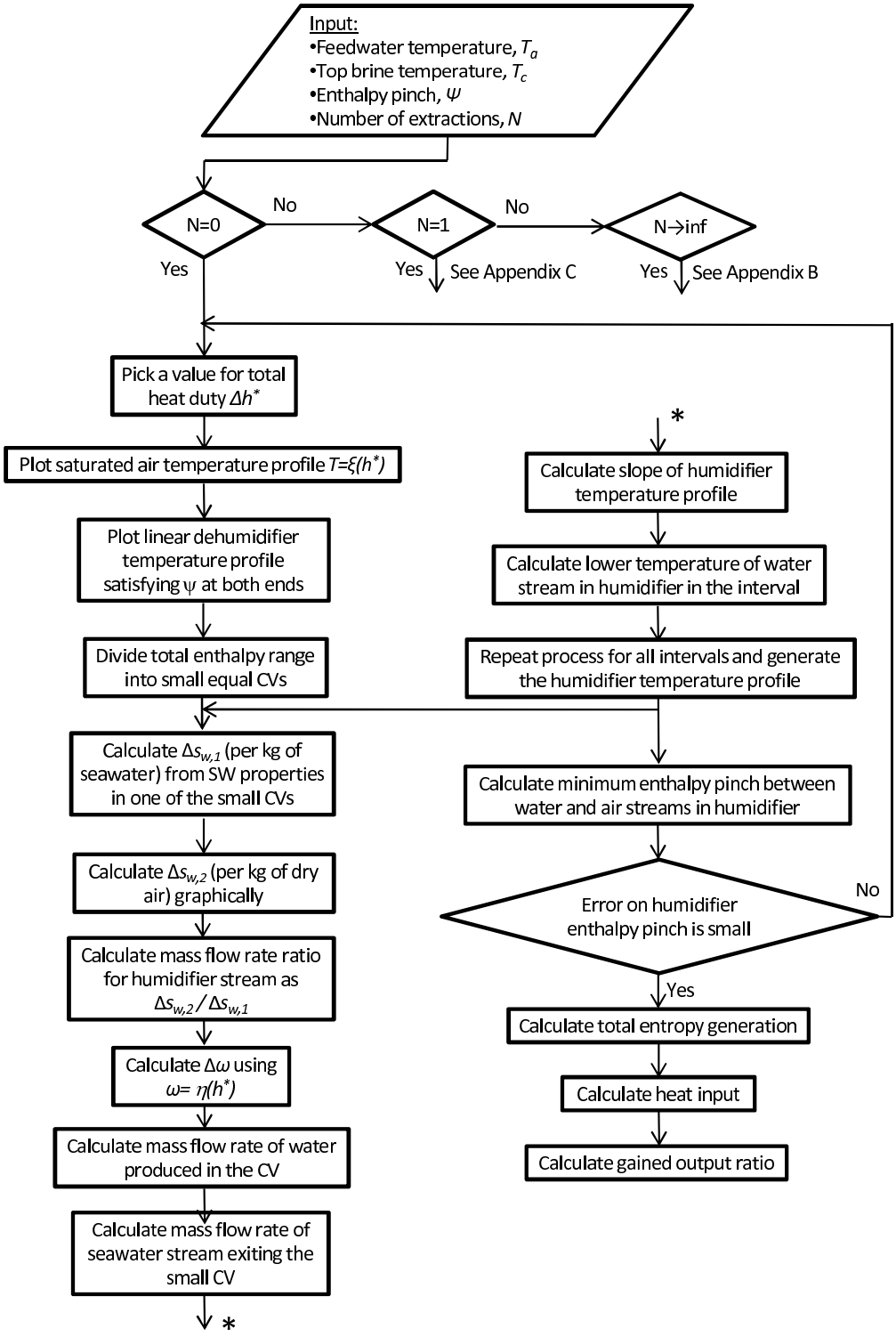

Figure 17: Flowchart of the overall HDH system design for the no extractions case.

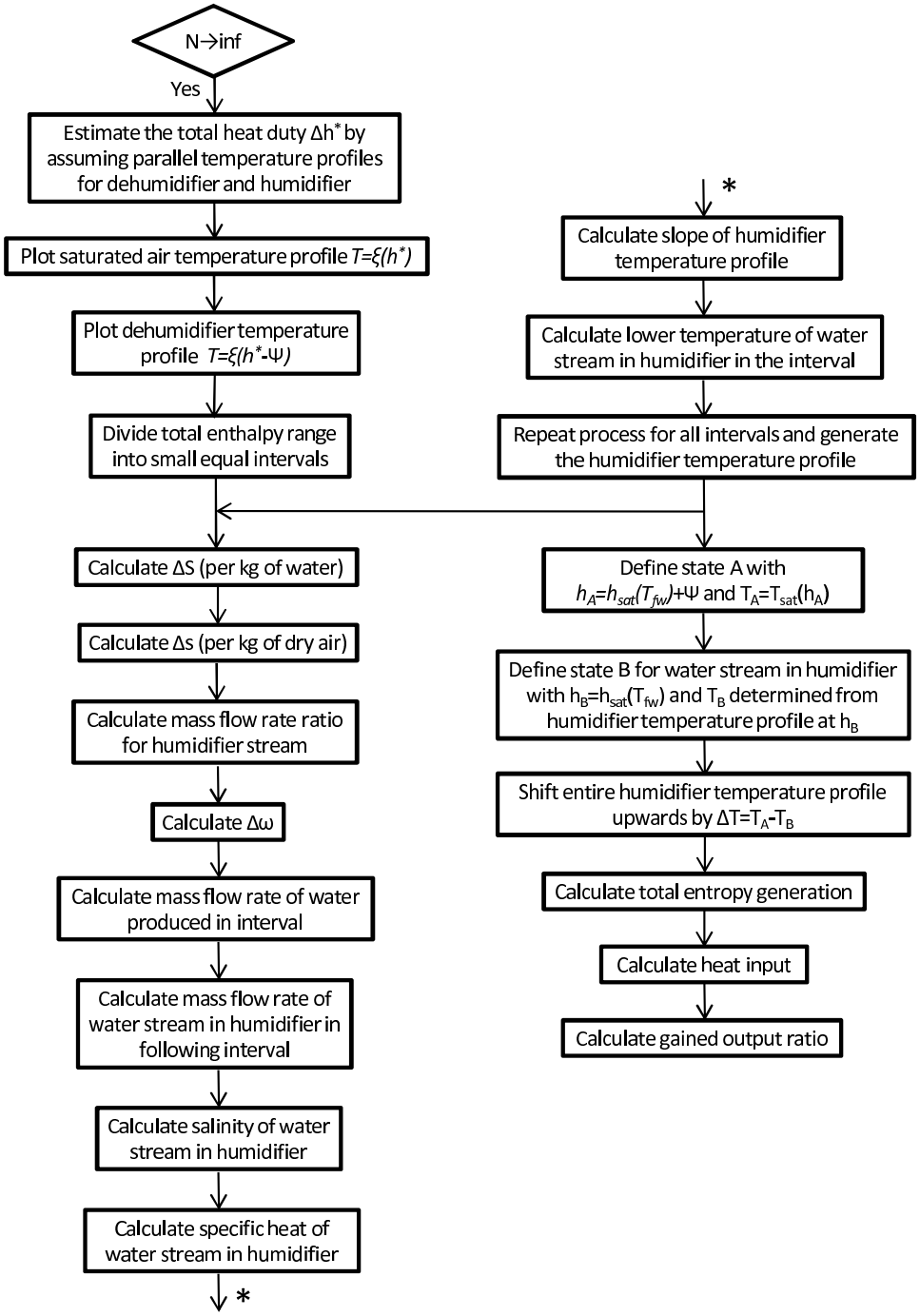

Figure 18: Flowchart of the overall system design for the continuous air extractions case.

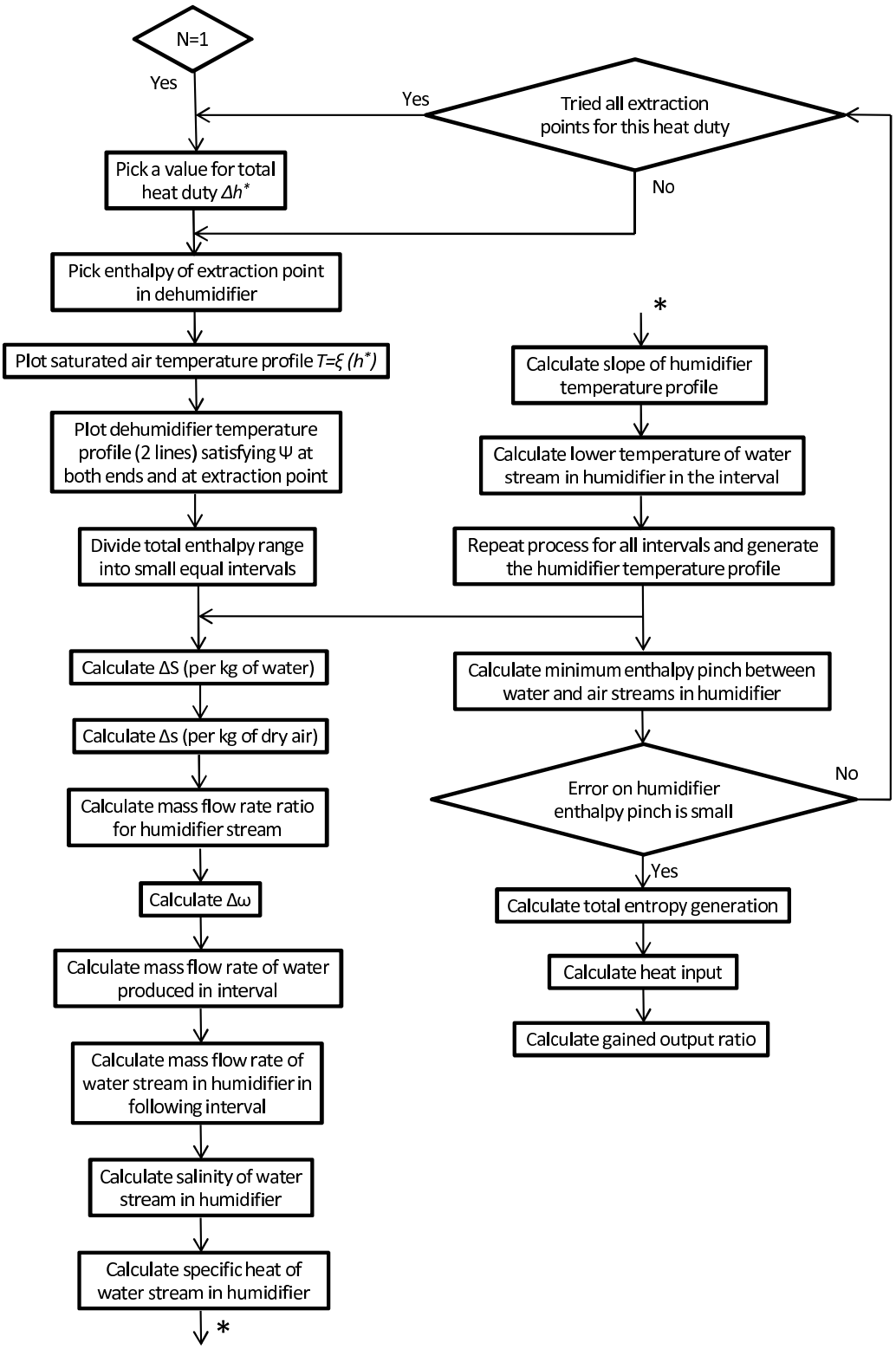

Figure 19: Flowchart of the overall system design for the single air extraction case.